

COMPUTATION AND ANALYSIS OF FLOW PATTERNS
IN THE SOLAR PHOTOSPHERE

by

RICHARD G. HENDL

B.S., Newark College of Engineering
1962

B.S., Pennsylvania State University
1963

M.S., University of Colorado
1968

SUBMITTED IN PARTIAL FULFILLMENT

OF THE REQUIREMENTS FOR THE

DEGREE OF DOCTOR OF

PHILOSOPHY

at the

MASSACHUSETTS INSTITUTE OF TECHNOLOGY

August, 1974

Signature of Author.....

Department of Meteorology
August 12, 1974

Certified by.....

Thesis Supervisor

Accepted by.....

Chairman, Departmental Committee
on Graduate Students

WITHDRAWN
FROM
AUG 28 1974
LIBRARIES

COMPUTATION AND ANALYSIS OF FLOW PATTERNS
IN THE SOLAR PHOTOSPHERE

by

Richard G. Hendl

Submitted to the Department of Meteorology
on August 12, 1974 in partial fulfillment
of the requirements for the degree of
Doctor of Philosophy

ABSTRACT

Almost all that is known about the velocity fields in the solar atmosphere pertains to mean quantities based on long periods of observation. Relatively little is known about short-term variations in both space and time which apparently exist and, according to some, ought to be basic to the maintenance of the solar general circulation. Only recently have theories which consider these variations to be energetically important been advanced to explain the solar circulation.

Evidence that short-term space and time variations do exist in the solar velocity fields is increasing; the primary source being the high resolution line-of-sight, Doppler derived velocity measurements made on a daily basis at Mt. Wilson Observatory. In the present work, these measurements from a two week period in 1972 have been utilized to produce nearly instantaneous horizontal streamline patterns depicting the large-scale flow in the solar atmosphere. The technique utilized is based on the assumptions that the flow is nondivergent and two dimensional. Included in the description are the various data processing and technique development experiments which led to the version ultimately selected.

The preliminary results from this analysis contain wavelike perturbations which persist for several days and rotate at nearly the solar rate. Additionally, the patterns resemble flows which are observed to occur in the earth's atmosphere as well as in laboratory simulations of flows in rotating fluids. Stronger evidence for accepting the reality of these flow patterns as first approximations of the actual flow in the solar atmosphere is provided by a significant correlation found to exist between meridional velocity components obtained from the flow patterns and from daily sunspot displacements.

Three pilot studies which serve to illustrate potential uses for these

data are discussed. An insufficient sample of data prevents reaching any definitive conclusions, but the results suggest the following: the existence of a loose relationship between calcium plages and small-scale flow features; a tendency for cyclonic vorticity to be found in the vicinity of active regions; and a tendency for the large-scale flow to transport momentum polewards and for this transport to be correlated negatively with the mean zonal velocity between $\pm 30^{\circ}$ latitude. Whether these results remain valid when applied to a larger data sample remains to be seen, but it appears that when perfected, daily maps of the solar velocity fields will represent an important new source from which to study the energetics of the solar circulation.

Thesis Supervisor: Victor P. Starr
Title: Professor of Meteorology

TABLE OF CONTENTS

ABSTRACT	2
LIST OF FIGURES	6
LIST OF TABLES	8
1. Introduction	9
1.1. The Solar Differential Rotation and Efforts to Explain It	9
1.2. Contribution and Scope of the Present Work	14
2. Obtaining Photospheric Streamlines from Solar Observations	18
2.1. Technique	18
2.2. Solar Data Utilized	21
2.3. Applicability of the Technique to the Solar Case	28
3. Producing Solar Flow Patterns	32
3.1. Introducing a Solid Body Reference	32
3.2. Minimizing the Effects of Small-Scale Convective Motions	33
3.3. Mechanics of the Analysis	44
4. How Well Does the Technique Work?	64
4.1. A Qualitative Assessment	64
4.2. A Quantitative Judgment	72
5. Applying the Flow Patterns to Solar Studies	91
5.1. Formation of Solar Activity Within the Large-Scale Flow	91
5.2. The Dynamics of Active Regions	99
5.3. Large-Scale Flow Patterns and the Solar General Circulation	102

6. Concluding Remarks	114
6.1. Summary	114
6.2. Suggestions for Future Work	120
APPENDIX A Velocity Components Relative to Integration Paths	123
APPENDIX B Calculation of Average Velocity in Annulus Due to Position of Sub-Earth Point	124
APPENDIX C Sunspot and Meridional Velocity Data	126
ACKNOWLEDGMENTS	128
REFERENCES	129
BIOGRAPHICAL NOTE	136

LIST OF FIGURES

Figure 1.	Solar coordinate system.	19
Figure 2.	Distribution of equivalent sectors over the solar disk.	41
Figure 3.	Center to limb variation in the mean Doppler velocity data determined for each annulus from all available measurements.	42
Figure 4.	Final data averaging configuration and location of the integration paths.	46
Figure 5.	Sample flow pattern which results when ψ_0 is assumed to be zero along the equator.	50
Figure 6.	Comparison of the flow patterns obtained when selecting ψ^* from the innermost and outermost integration paths.	57
Figure 7.	Comparison of the flow patterns obtained from streamfunction calculations starting on the equator in the eastern and western hemispheres.	59
Figure 8.	Comparison of the flow patterns obtained from equivalent sectors divided into 4, 8, and 12 equal parts prior to averaging.	62
Figure 9.	Final version of the flow patterns for the period 30 June - 14 July 1972.	65
Figure 10.	Scatter plot comparing meridional velocity components obtained from the flow patterns with those inferred from the daily proper motion of sunspots.	87
Figure 11.	The location of calcium plages and sunspots in the large-scale flow patterns.	93

LIST OF FIGURES (continued)

- Figure 12. Flow in the vicinity of an active region inferred from various solar measurements 103
- Figure 13. The day to day variation in the mean values of the zonal velocity between $\pm 30^\circ$ latitude and the covariance between the zonal and meridional velocity components at $\pm 30^\circ$ latitude. 108
- Figure 14. The day to day variation in the mean values of the zonal velocity between $\pm 30^\circ$ latitude and the covariance between the zonal and meridional velocity components which lie in the latitude belt bounded by 10° and 30° in both hemispheres. 109

LIST OF TABLES

Table 1.	Sample distribution of data points within annular rings representing multiples of equal surface area.	37
Table 2.	Sample distribution of data points within annular rings representing multiples of equal disk area.	38
Table 3.	Sample distribution of data points within annular rings of equal width.	40
Table 4.	Values of the streamfunctions at the western and eastern hemisphere equators which result after completing half an integration path assuming $\psi_0 = 0$ on the equator.	44
Table 5.	Change in the value of ψ^* on successive integration paths corresponding to the mean net circulation observed in each annulus when $B_0 \neq 0$.	56

1. Introduction

1.1. The Solar Differential Rotation and Efforts to Explain It

Prior to 1964 the only documented variation in the solar rotation rate was a function of latitude. This "differential" rotation was first observed by Carrington in 1863 and refined over the following nine decades culminating in the form obtained by Newton and Nunn (1951). Their result was based on the interval between successive central meridian passages for long-lived, recurrent sunspots from six solar cycles and essentially confirmed Carrington's initial finding -- the solar rotation rate was solely a function of latitude.

Newton and Nunn were aware that their particular subset of sunspots produced a result which differed from those obtained from other subsets, but they judged the long-lived recurrent spots to be the most reliable tracers of the photospheric motions. Velocity profiles obtained using spectroscopic methods (Plaskett, 1952, 1954, 1959; Kinman, 1953; Hart, 1954, 1956; Adam, 1959) while agreeing with the sunspot rotation rates in the mean, contained the suggestion that the solar rotation rate was not as longitudinally invariant as the accepted profile would suggest.

Theories attempting to explain the differential rotation which had evolved concurrently with the observations were generally based on this axisymmetric picture and reproduced the observed equatorial acceleration. Such theories appeared to be adequate when considered in a mean qualitative sense, but were deficient in most quantitative aspects.

A new approach to the subject was suggested by Ward (1964, 1965a) who viewed the mean solar rotation as the largest of a continuous spectrum of size and velocity scales. Scales of motion smaller than this, he asserted, should not be viewed as noise to be averaged out; rather they are fundamental to the energetics of the solar circulation. Ward postulated the existence of a hierarchy of eddies in the solar atmosphere ranging in size from a fraction of the solar radius to a few hundred kilometers and sufficiently organized in space and time to maintain the mean circulation.

Citing results from laboratory experiments and analogous situations in the earth's atmosphere, Ward argued for the existence of a Rossby circulation regime in the solar atmosphere. As corroborating evidence for this contention, he analyzed the daily proper motions of sunspots for one solar cycle and obtained positive correlations between deviations from the space and time averaged meridional and zonal components of these motions. Such a correlation, Ward concluded, implies a horizontal transport of angular momentum up the angular velocity gradient (towards the equator), a phenomenon known to exist in the earth's atmosphere (e.g., Starr, 1968). The circulation pattern associated with such a transport requires a solar rotation rate which varies in space or time or both.

Starr and Gilman (1965a, b) utilized Ward's findings in addition to maps of the photospheric magnetic field to infer the direction and

magnitude of the angular momentum transfer as well as to speculate on the shape and orientation of perturbations in the zonal flow field. Such a process could be similar to those which maintain the circulation of the earth's atmosphere and generally cause marked deviations from mean conditions in both space and time. They further speculated that horizontal Maxwell stresses converting the energy of the mean flow into the energy in the large scale magnetic patterns were acting to retard the equatorial acceleration. The net transport represents a balance between competing processes.

Since then, the evidence to support the contention that the solar rotation varies in space and time has been accumulating from other sources, e.g., magnetic field data (Wilcox and Howard, 1968; Wilcox and Colburn, 1969; Stenflo, 1972) and velocities obtained from Doppler shifts (Plaskett, 1966; Howard and Harvey, 1970; Howard, 1971, 1972, 1973).

Despite the recent evidence to the contrary, there are those who continue to maintain that the deviations from the mean solar rotation are not basic to the underlying energetics. These variations continue to be ignored even though their magnitude approaches that of the differential rotation itself. Such theories continue to rely on an axisymmetric circulation regime but unlike similar theories in the past, the meridional circulations are not constrained to conserve angular momentum. These models are based on the assumption that motions experience certain

anisotropies in basic properties, e.g., eddy viscosity (Kippenhahn, 1963; Cocks, 1967), conductivity (Durney and Roxburgh, 1971). These anisotropies as modeled produce meridional circulations transporting angular momentum towards the equator. However, all are characterized by an eddy viscosity and require negative viscosity coefficients at some point to produce consistent energetics (Gilman, 1974). Some parameterizations introduce into the mathematical model the necessary effects of eddies while not fully exploring the physical implications. The resultant pitfalls of this approach have been discussed recently by Starr (1973a).

Other recent attempts to explain the maintenance of the solar differential rotation are based on investigations of the full eddy regime. These theories tend to be more quantitatively well developed than the axisymmetric type. Two mechanisms are considered; the distorting effect of rotation on "giant" convective cells (Kato, 1969; Busse, 1970; Davies-Jones and Gilman, 1970; Yoshimura, 1971; Gilman, 1972; Heard and Veronis, 1974) while the other considers the presence of baroclinic instabilities (Gilman, 1969; Kato and Nakagawa, 1969, 1970; Suess, 1971). Both types successfully reproduce the observed equatorial acceleration and transport angular momentum towards the equator. For the assumed geometry and physical parameters, both mechanisms produce large-scale features with dimensions in general agreement with those inferred both from Doppler velocity measurements (Howard, 1971) and from photospheric magnetic fields (Starr and Gilman, 1965b). The

particular shape (longitudinal rolls) of this large-scale feature suggested by the Doppler velocity measurements presently favors the giant cell models (Piddington, 1971; Gilman, 1972) although Suess (1971) has interpreted these same patterns in terms of Rossby-type waves. Observed whole sun magnetic variations, e. g., field reversals, have been modeled with some success utilizing a dynamo based on Rossby wave dynamics (Gilman, 1969; Gordon, 1972).

Encouraging as the results of such models are, they are not without their shortcomings. Generally the assumptions made in order to solve the complex systems of equations place restrictions on the character of the solutions to the extent that their applicability to the sun is uncertain at best. More explicitly, the models either assume or produce certain features which, if present, ought to be evident from the available observations. One example of such a feature which pertains to both theories is the presence of an equator to pole temperature gradient. The Rossby wave theories usually assume the existence of such a gradient to provide the energy for the resulting instability (Gilman, 1969) while the giant cell theories produce such a temperature gradient (Davies-Jones and Gilman, 1970; Gilman, 1972). The gradient in either case is approximately 50K and most recent measurements fail to confirm its existence (Altrock and Canfield, 1972; Canfield, 1973). Durney (1972, 1974) maintains that the pole-equator difference in flux produced by the convective models would occur deep in the convection zone but would be unobservable at the

surface due to a reduction by a counter cell higher up rising at the poles and sinking at the equator. At least one Rossby wave model exists (Kato and Nakagawa, 1969) which does not assume the existence of a temperature gradient. Instead, the waves are considered to be perturbations relative to a system rotating at a constant rate.

The mean meridional circulation characteristic of the giant cell models presents another discrepancy; most models contain a mean equatorward flow (Gilman's is poleward). The observational measurements of mean meridional velocities either from sunspot data (Ward, 1964, 1973) or Doppler velocity data (Howard, 1971) have not yielded such circulations although the Doppler measurements are not sufficiently precise to detect motions of the magnitude required ($\sim 3\text{m} - \text{sec}^{-1}$).

Clearly, all the theories proposed to explain the energetics of the solar general circulation cannot be entirely correct. Some combination is likely, for example, with convection in the interior producing a baroclinically unstable layer at the surface (Starr, 1973b). Such a system would combine a pole to equator temperature gradient (in this case at some level below the visible surface) produced by the giant convection cell theories with the non-axisymmetric flow characteristic of baroclinic instabilities. This particular combination would not violate any observations as they are presently accepted.

1.2. Contribution and Scope of the Present Work

As pointed out in the previous section, each theory developed to

explain the solar general circulation contains one or more features which has not been observed in the solar atmosphere. Unfortunately, the measurements of solar features are not themselves without difficulties. Efforts to observe a pole to equator temperature difference are made more difficult by the lack of assurance that the optical solar limb is also a surface of constant heliopotential. Alternatively, if a dynamically important temperature difference exists in the solar interior, direct observation will be impossible.

One of the major problems still existing is the lack of sufficient observations of the motions (particularly meridional) which exist in the solar atmosphere. Even the mean rotation rate, first observed over a century ago, is no longer a sufficient description of motions in the photosphere much less the entire sun. There is probably no one rotation rate which can be applied to the sun as a whole since the mean conditions appear to vary with depth in the atmosphere (Wilcox and Howard, 1970). Even less well known are the short-term variations in latitude, longitude and time (Livingston, 1969; Howard and Harvey, 1970; Howard, 1971, 1972, 1973) which are relatively recent determinations.

Instantaneous horizontal velocities can be obtained from motions of visible tracers and (at least theoretically) from Doppler shifts of spectral lines due to mass motions along the line-of-sight. Each technique has its own shortcomings which contribute to the uncertainty of the results. The difficulties encountered when attempting to determine instantaneous velocity

fields from sunspots are more acute than when determining mean motions. These include the lack of a sufficient number of tracers at a given time, non-random distribution of sunspots in the flow field and the probable retardation of sunspot motions due to the presence of a magnetic field and the interchange of matter between sunspot and flow field. Further complexity is introduced since the degree to which sunspots fail to be ideal tracers varies with solar cycle and the stage of sunspot development (for a more complete discussion see Ward, 1965b; 1966a, b; 1967; 1973). Velocities obtained spectroscopically are free from these limitations. However, the technique is accompanied by its own particular difficulties (Howard et al., 1968) which will be examined in more detail in following sections.

The lack of sufficiently well determined motions in the solar atmosphere has contributed to the variety of solar circulation theories which have emerged. The basic difference between the non-axisymmetric theories and those based on primarily axisymmetric flows concerns the relationship between space and time deviations from the mean solar rotation rate and the underlying energetics. Proponents of the axisymmetric theories minimize the importance of deviations, providing mechanisms to maintain the equatorial accelerations from mean circulation regimes. On the other hand, proponents of non-axisymmetric theories accept the existence of significant space and time variations in the solar rotation rate and assign to these deviations major roles in maintaining the mean circulation.

The energy associated with these variations in the rotation rate are orders of magnitude greater than that associated with other available forms, e.g., magnetic energy. If such variations are fundamental to the energetics of the solar circulation, there will be detectable relationships which exist between the large-scale flow pattern and other observable features.

The scope of the work described herein is to obtain for the first time instantaneous large-scale flow patterns in the solar photosphere as they are inferred from daily Doppler line-of-sight velocity measurements. A description of the analysis technique, the preliminary data processing and the experiments performed to bridge the gap from theory to practice are contained in the following two chapters.

Daily flow patterns for a two week period in 1972 are presented and discussed in the fourth chapter which also contains more quantitative judgments of their overall validity based on comparisons with observations of other solar phenomena. Estimates of the momentum transports associated with the flow characterization are related to the observed variations in the daily determined mean rotation rate. The implications of these results as they pertain to the energetics of the solar general circulation along with suggestions for future research are the topics of the final chapters.

2. Obtaining Photospheric Streamlines from Solar Observations

2.1. Technique

Velocity fields in the solar atmosphere may be obtained by measuring Doppler shifts in selected Fraunhofer lines. These Doppler shifts are due to motions within the line forming layer along the line-of-sight and as such render invisible components of the motions which are normal to this direction. When viewed from the earth, purely horizontal and vertical solar motions are undetectable at the central meridian and limb respectively. Alternatively, the line-of-sight velocity contains an increasing portion of a purely horizontal velocity field as the observation approaches the solar limb.

A technique to infer the continuous horizontal flow field from this type of photospheric velocity measurement has been suggested by Gilman (1971). Basically, the procedure assumes the flow along the solar surface to be horizontal, two-dimensional and nondivergent. Momentarily setting aside questions concerning the applicability of such assumptions, the horizontal divergence can be expressed, following Gilman, as:

$$\frac{\partial V_{\lambda}}{\partial \lambda} + \frac{\partial (V_{\theta} \cos \theta)}{\partial \theta} = 0 \quad (1)$$

where V is the velocity and λ and θ denote the solar central meridian distance and latitude respectively (see Figure 1). A streamfunction Ψ may be defined such that

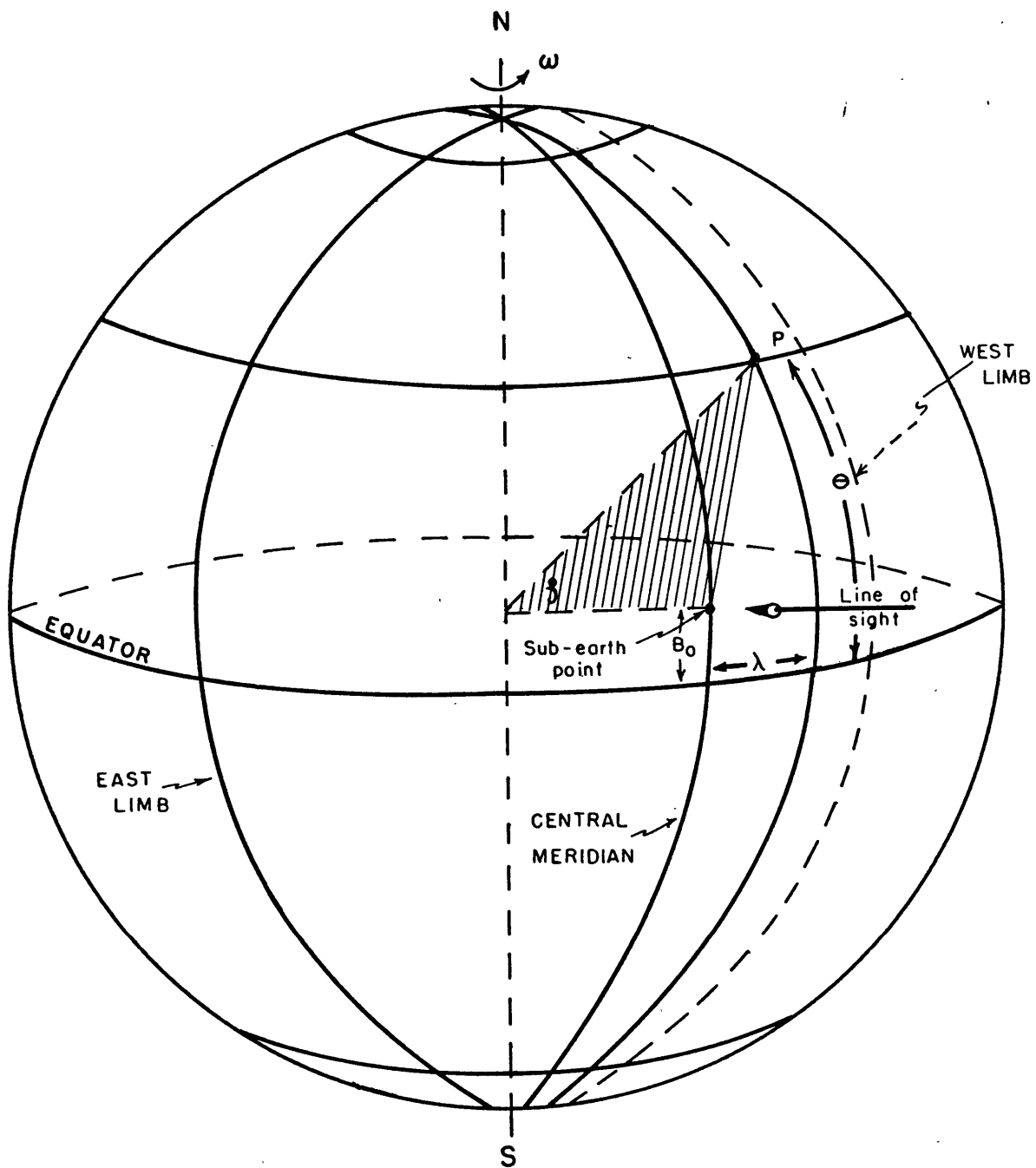


Figure 1. Solar coordinate system.

$$V_{\lambda} = -\frac{\partial \psi}{\partial \theta} ; \quad V_{\theta} = \frac{1}{\cos \theta} \frac{\partial \psi}{\partial \lambda} \quad (2)$$

The line-of-sight velocity, V_{ℓ} , is related to V_{λ} and V_{θ} by:

$$V_{\ell} = -\sin \lambda V_{\lambda} - \sin \theta \cos \lambda V_{\theta} \quad (3)$$

or

$$V_{\ell} = \sin \lambda \frac{\partial \psi}{\partial \theta} - \tan \theta \cos \lambda \frac{\partial \psi}{\partial \lambda} \quad (4)$$

which upon integration becomes

$$\psi = \psi_0 + \int_S V_{\ell} ds \quad (5)$$

The paths of integration are such that

$$\cos \lambda \cos \theta = \text{constant} \quad (6)$$

which for the sun are circles centered on the sub-earth point.

In equation (5), the constant of integration ψ_0 is unspecified and differs for each integration path S . In order to produce a continuous solution for the entire solar disk, these arbitrary constants must be related to one common but still unspecified constant. Gilman suggested as a first approximation that ψ_0 be set equal to zero along the equator. Such a stipulation prohibits flow across the equator.

A test of the technique was performed on terrestrial wind data by Fischer (1971). Utilizing six month summertime mean wind components for the half of the northern hemisphere centered on the Atlantic Ocean, he computed the line-of-sight velocity component apparent to an extraterrestrial observer and used Gilman's technique to infer the streamline pattern.

Direct application of the procedure resulted in small non-zero values for Ψ at the termination of each integration path (semi-circular in this case) and were attributed to the presence of a small divergent component, cross-equator flow or both. It was not possible to estimate the contribution due to each but their effect was removed by subtracting the mean wind from the data. Overall agreement between the actual mean wind field and the flow patterns produced by the technique was favorable, encouraging its extension to an analysis of solar velocity fields.

2.2. Solar Data Utilized

Forming the basis for this work are instantaneous line-of-sight velocities inferred by measuring Doppler shifts in the neutral iron line (FeI) at $\lambda 5250.216$ formed in the solar photosphere. Daily whole disk measurements are made at Mt. Wilson Observatory and have been described in a series of papers (Howard et al, 1968; Howard and Harvey, 1970; Howard, 1971, 1972). These measurements are configured in a rectangular grid 135 points wide, 108 points high of which approximately 11,000 points actually sample the solar disk. Resolution at each grid

point is approximately 0.17 seconds of arc while the distance between grid points is roughly one and a half degrees of solar latitude.

Doppler shifts when observing a solar spectral line from the earth occur whenever relative motion exists between the observing instrument and the volume of gas in which the line originates. Not all motions which contribute to the observed shift originate in local velocity fields on the sun. The rotation of both the earth and sun as well as the orbital motion of the earth contribute to the observed Doppler shift. In addition, the reddening of a solar spectral line as it is observed progressively limbward contributes an apparent shift as do a variety of instrumental effects. A complete discussion of the instrumental contributions appears in Howard and Harvey (1970) and will not be considered here. However, it is instructive for a better understanding of the streamline patterns being sought to review briefly how these and other contributions to the observed Doppler shift are removed before the resulting motions can be attributed to the solar atmosphere.

The line-of-sight velocity V_L obtained from the observed Doppler shift in the FeI line is assumed to be the combined effect of relative motions (real or apparent) between the line-forming layer and the observing instrument and are accounted for by Howard and Harvey (1970) as the sum of individual contributions in the following manner:

$$V_d = \overbrace{(a + b \sin^2 \theta + c \sin^4 \theta)}^{(1)} R \cos \theta \cos B_0 \sin \lambda$$

$$+ \overbrace{0.38511 \sin H \cos \delta}^{(2)} - \overbrace{29.789 \sin(L_0 - L)}^{(3)} + \overbrace{d}^{(4)} + \overbrace{e(1 - \cos \varphi)^2}^{(5)} + \overbrace{V_{SM}}^{(6)} \quad (7)$$

A description of the origin of each term follows.

① Contribution from the mean solar rotation

The mean solar rotation is one of the quantities under current investigation at Mt. Wilson Observatory. It is determined on a daily basis along with several other parameters by evaluating the constants a , b , and c from each day's measurement. The long term value is the mean of the individual values for the period of determination. The functional form for the latitudinal dependence is guided by the differential rotation profiles obtained from sunspot motions. Term ① in Equation (7) represents the component of the mean solar rotation in the line-of-sight. Other quantities previously undefined are R , the radius of the sun and B_0 , the heliographic latitude of the sub-earth point.

② Contribution from the earth's rotation

If the observation is taken prior to local noon, the rotation of the earth produces a slight component of motion towards the sun. Observations made after local noon contain the reverse effect. The appropriate component in the line-of-sight is proportional to the well known astronomical constants H , the hour angle at observation time, and δ the declination of the line-of-sight with respect the ecliptic plane. Knowing

the date and time of the observation as well as the geographic location of the observatory are all the quantities necessary to calculate this component of relative motion. Sufficiently precise determinations of this component are obtained by basing all calculations on a mean sidereal day.

③ Contribution due to the orbital motion of the earth

Both ecliptic plane components of the orbital motion contribute a relative sun-earth motion. The earth-sun distance varies throughout the year resulting in a small day to day relative motion. Over the 90 minute interval required to take an observation this motion is below the limits of detectability and is ignored. The tangential component represents the difference between synodic and sidereal rotation rate of the sun and is represented by term ③ with L_0 and L the celestial longitude of the center of the solar disk and line-of-sight, respectively. The earth's orbit around the sun is assumed to be a perfect ellipse with the sun at one focus. Other minor effects which have been neglected are the seasonal variations in the linear sidereal velocity of the earth in its orbit and the celestial latitude of the line-of-sight, B . This latter effect would be represented by an additional factor, $\cos B$, in term ③. However, since B is always near zero degrees, $\cos B$ is assumed always to equal one. As was true for the preceding term, the relative motion between the earth and sun due to the earth's orbital motion can be calculated from known astronomical quantities and is not determined as a result of the observation.

④ Reference level

In its present version, the Mt. Wilson instrument measures the wavelength shift in the FeI line only. If this shift was entirely due to local motions on the sun (after accounting for the other known effects), the absolute velocity between the plasma and the observer would be directly proportional to the observed line shift. Unfortunately, the shift as measured contains unknown contributions from the terrestrial atmosphere and instrumentation. These effects must be removed before the velocities in the solar atmosphere are estimated. This removal is accomplished by determining a reference level, term ④, which represents the aforementioned effects on an observation of a stationary sun. The individual measurements are then reckoned with respect to this reference level.

To be effective, this reference level should remain constant over the span of time required to make the observation. The overall contribution to the noise attributable to mechanical components, e. g., backlash, ought to be near zero due to the boustrophedonic nature of the scan. More troublesome may be a net drift in this reference due to changes in atmospheric pressure during the course of an observation. A change of 0.1 mm Hg in pressure produces a drift in the reference of nearly $60 \text{ m} - \text{sec}^{-1}$. This effect would tend to produce a random noise component in studies dependent on averaging many measurements over a long period to determine, say, the long term mean rotation rate. Since these observations were made with such long term determinations in mind, no

pressure correction was made and its effect on daily measurements is unknown.

A future improvement which will allow a direct determination of the portion of the line shift which is not solar in origin is the simultaneous monitoring of a nearby spectral line which is formed in the earth's atmosphere. Any shifts in the wavelength of the telluric line is then attributed to atmospheric and instrumental effects. A corresponding correction is applied to the solar line at each point which removes all non-solar contributions from the measurements and allows absolute velocities to be determined.

⑤ Red shift contribution

It is well known that the wavelength of a solar spectral line shifts towards the red as the observations are taken at points progressively nearer the limb. This center to limb variation (which is actually a blue shift towards the center) was originally thought to be due to preferential sampling of warm convecting elements. Such an explanation requires a center to limb variation proportional to $(1 - \cos \varphi)$, where φ is the central angle. Observations, however, did not support this contention. Instead, Adam (1959) found the best fit was obtained assuming a parabolic proportional to $(1 - \cos \varphi)^2$. This functional form is used in the Mt. Wilson data reduction technique to predict the degree of red shift to be expected in the data. The unspecified constant, e , like those preceding is determined by the daily data.

The entire limb reddening variation is undergoing a careful re-examination by Hart (1974) utilizing the vast amount of data resulting from the Mt. Wilson observing program. A new theory is being tested which contends that the line shift observed is due to the combined effect of Van der Waals and Lennard-Jones potentials. Such an effect is proportional to the density of the environment in which the line originates and in the case of the sun would produce a shift to the blue at the center of the disk since the radiation originates from deeper and therefore denser levels. The wavelength variations from center to limb predicted for selected spectral lines have produced better agreement with the observations than the $(1 - \cos \varphi)^2$ form presently used.

⑥ Motions in the solar photosphere

The final term, V_{SM} , represents the velocity component due to deviations from the daily profile of the mean rotation. If the daily zonal velocity field, u , is decomposed into its mean value $[u]$ and deviations (u'), i.e.,

$$u = [u] + u' \quad (8)$$

term ⑥ represents the u' component, $[u]$ already being accounted for by term ① in Equation (7). Also included in V_{SM} are the line-of-sight components of any meridional and vertical (radial) motions which may be present.

The daily array of observations is analyzed by a least squares technique with V_{SM} treated as a residual. Once a solution is obtained and

the daily values for constants a through e determined, V_{SM} is calculated for each grid point. The daily data obtained from Mt. Wilson Observatory consist of values for V_{SM} at each grid point as well as for the constants a , b , c , and e . Solutions are obtained determining the rotation rate constants for the northern and southern hemispheres independently as well as for the disk as a whole.

A data reduction technique of this type is well suited to a study of the mean rotation rate but has certain disadvantages when subjected to a day by day analysis such as that attempted by the present study. Since V_{SM} is treated as a residual, it also contains any noise components, random and non-random, which remain if the foregoing considerations have been insufficiently precise. Any unconsidered effects traceable to variations in atmospheric transparency and instrumental sources would probably alter the reference level in a uniform manner and produce little effect in the data for a given day. On the other hand non-random contributions, for example, the drift in the reference point due to changes in atmospheric pressure, would produce a slightly inhomogeneous data set during the 90 minutes it takes to obtain a complete disk scan. The mean of such a variation would become part of the reference level but a small non-random component could remain behind.

2.3. Applicability of the Technique to the Solar Case

Before proceeding further with a description of the steps involved in producing daily flow patterns from solar line-of-sight velocity

measurements, a consideration as to the applicability of the technique to the solar case seems appropriate.

At first glance the assumptions upon which the technique is based, namely horizontally two-dimensional and nondivergent flow appear vastly inadequate to faithfully represent motions in the solar photosphere. It is well accepted that the solar photosphere is primarily a convective layer from which radiation is being lost to space so rapidly that energy must be transported by convective rather than radiative processes. The theoretical criterion for stability against convection (Aller, 1963) is

$$\left[\frac{d(\ln T)}{d(\ln P)} \right]_{\text{PHOTOSPHERE}} < \left[\frac{d(\ln T)}{d(\ln P)} \right]_{\text{ADIABATIC}} \quad (9)$$

From models of the photosphere (c.f., Allen, 1963) this criterion is generally met only for the uppermost layer of the photosphere between optical depths $\tau \sim 0.004$ (defining the base of the chromosphere) and 0.8 (~ 280 km below). It is in this thin, stable layer where the Fraunhofer lines are formed.

Undoubtedly, the actual conditions are not as orderly as a model of the photosphere would suggest. Convection from below most likely penetrates the underside of the stable layer and induces vertical motions within it much like tropospheric convection penetrates into the stratosphere.

While the density is not discontinuous at the top of the photosphere, it falls off rapidly enough throughout the lower layers of the chromosphere

to enable the surface of the sun to be treated as a free surface with no flow across it. When dealing with sub-sonic motions in the solar photosphere, the flow may be treated as incompressible (Nakagawa and Priest, 1973).

Expanding the vertical component of motion in terms of a mean taken around latitude circles ($[\]$) and deviations therefrom ($'$), the continuity equation becomes

$$\frac{\partial u}{\partial x} + \frac{\partial v}{\partial y} + \frac{\partial w'}{\partial z} = 0 \quad (10)$$

since $[\omega] \approx 0$.

If motions on the scale of the convection are being considered, Equation (10) would have to be applied as written. However, the intent of this analysis is to depict the large scales of horizontal motion assuming that there is no ordered vertical motions with so large a scale. The additional assumption is made that if the scale of the substantive convection can be identified, the data representing an area occupied by several cells can then be averaged (\wedge) such that the resulting value contains very little contribution from the smaller scale convection, i.e., $\hat{\omega}' \approx 0$.

Thus, if the radiation yielding the measurements originates fairly high in the photosphere near $\tau \sim 0.004$ the assumptions that the flow is horizontally two-dimensional and nondivergent are generally good ones. On the other hand if the radiation originates in deeper layers near the top

of the convection zone ($\tau \sim 0.8$), the forcing by the strong underlying vertical motions may weaken the validity of those assumptions if the measurements are capable of resolving the convection.

A mean optical depth τ_0 can be defined such that one-half the radiation emerging from the surface originates above and one-half below this level. For a grey atmosphere, $e^{-\tau_0} = 1/2$ or $\tau_0 \sim 0.69$. Therefore, most of the radiation observed by the instrument originates slightly above the top of the convective zone and probably includes motions influenced by the underlying convection. The success of the technique in representing the large-scale velocity fields in the solar photosphere will depend in large measure on successfully removing the effects of this smaller-scale convection from the mean line-of-sight velocity data ultimately used to calculate the streamfunctions.

3. Producing Solar Flow Patterns

3.1. Introducing a Solid Body Reference

The intent of this analysis is to construct large-scale flow patterns for the solar photosphere analogous to those depicted on constant pressure charts representing flow in the terrestrial atmosphere. This similarity is desirable to facilitate the interpretation of the results, especially with an eye towards identifying any structure which may exist in the space and time variations from the mean solar rotation rate which these Doppler data seem to contain. In order to achieve such a product, it is necessary to refer the velocity fields in the solar atmosphere to an underlying solid body rotation rate.

The measurements as obtained from Mt. Wilson Observatory represent the line-of-sight components of velocities in the solar photosphere except for that component arising from the daily mean rotation rate. However, this mean itself changes from day to day (as the daily variation in a , b , and c indicate) and in doing so contributes to any variability present. In order to achieve the stated objective a common reference must be selected.

At first glance, the rotation rate of the Greenwich coordinate system appears to be the obvious choice. However, this coordinate system reflects a mean rotation rate characteristic of recurrent sunspots which differs somewhat from that obtained by spectrographic methods. Rather than use a reference characteristic of another level, it was decided to

utilize the long-term mean rotation rate determined from the spectroscopic data themselves. This mean rotation rate is (Howard and Harvey, 1970)

$$\overline{[\omega_{\theta}]} = 2.78(10^{-6}) - 3.51(10^{-7}) \sin^2 \theta - 4.43(10^{-7}) \sin^4 \theta \quad \text{sec}^{-1} \quad (11)$$

An overbar ($\overline{\quad}$) will be used to denote a time average. As an underlying reference, the angular frequency of rotation corresponding to $+20^{\circ}$ was selected

$$\overline{[\omega_{20^{\circ}}]} = 2.73(10^{-6}) \quad \text{sec}^{-1} \quad (12)$$

The V_{sm} , data were then adjusted point by point to re-introduce the line-of-sight component ΔV_{ℓ} due to the difference in the daily and long term mean rotation rates. This adjustment was straightforward

$$\Delta V_{\ell} = R \left(\overline{[\omega_{\theta}]} - \overline{[\omega_{20^{\circ}}]} \right) \cos \theta \sin \lambda \cos B_0 \quad \text{m-sec}^{-1} \quad (13)$$

Adhering to the Mt. Wilson sign convention, ΔV_{ℓ} is negative for approach and positive for recession. Defining solar velocities in this manner produces in the mean westerlies equatorward and easterlies poleward of $+20^{\circ}$ heliographic latitude. Directions here are reckoned in a terrestrial sense, i.e., zonal velocity fields in the same sense as the rotation are referred to as "westerlies". As will be discussed in more detail in sections to follow, the solar rotation rate for the period analyzed is greater than average resulting in a substantial poleward displacement of the boundary separating easterlies and westerlies.

3.2. Minimizing the Effects of Small-Scale Convective Motions

In section 2.3 it was concluded that if a suitable area could be defined which would include more than one of the underlying convection cells,

the line-of-sight velocity data within this area could be averaged and the mean value contain little, if any, contribution from the vertical motions organized on the smaller scale. Prior to exploring the scale size of the convection present in the solar atmosphere, a determination of how best to uniformly represent various portions of the solar surface must be made.

Ideally, the solar surface should be uniformly sampled to avoid over-representing one portion of the hemisphere while neglecting others. Clearly this ideal goal is unattainable since the geometric realities of observing a sphere from a fixed point in space will always provide more direct access to that portion of the surface directly beneath the vantage point. For example, the half of the surface area lying limbwards of 60° central angle is represented by slightly less than 25% of the area of the solar disk (the apparent area covered by any earth-based measurements).

Furthermore, the Doppler measurements suffer from an additional asymmetry. A given line-of-sight velocity contains a more direct measurement of actual horizontal motions when obtained near the limb than it does near the center of the disk. Therefore, the chance for contamination by vertical motions is greater at the center than towards the limb. When representative line-of-sight values for the large-scale motion are being produced, more data points should be used to compute the mean near the center per unit surface area than near the limb to obtain values with similar residual effects. So the initial step in the averaging procedure is to decide how best to produce homogenous means which represent

roughly the same surface areas.

A practical consideration to the ultimate averaging technique was the circular geometry required to calculate the streamfunctions. It was necessary to provide mean values for the line-of-sight velocities on circular paths centered on the sub-earth point. Such a final configuration is directly achieved by dividing the disk into annular rings, then the rings azimuthally in some regular fashion and assigning the mean value of all data within each sector to the sector center of gravity. Alternatively, primary averaging could be accomplished maintaining a rectangular grid, then values obtained along circular paths by interpolation. Both approaches were tested and yielded similar results for identical integration paths. The purely circular method was preferred since it weighted each data point equally in producing the mean for the sector it represented while for the rectangular technique it was not clear how this could be accomplished while maintaining a truly independent procedure. Additionally, the circular method is easily related to the fraction of the surface area falling within each sector, a distinct advantage in the analysis which follows.

Once having decided (albeit somewhat arbitrarily) on the geometrical form the averaging procedure will assume, the question concerning how best to represent the entire solar surface can be pursued. It has already been stated that while most desirable, strictly uniform sampling of the solar atmosphere for the entire solar hemisphere is unattainable. However, this does not prevent one from dividing the solar surface into

equal portions and utilizing the measurements which happen to fall within the projection of each to provide a mean value for each equal portion. This approach would assure that a large number of data points were averaged over segments near the sub-earth point while fewer would determine the mean near the limb. This approach need not provide a realistic representation of motions towards the limb since the distribution of data points results in over-sampling the portions near the center of the disk while those portions near the limb are sparsely sampled or occasionally sampled not at all.

To be more specific, Table 1 contains, for the data distribution used in this study, the number of measurements per unit surface area as a function of central distance. The unit surface area was defined by dividing the solar hemisphere into ten annular rings concentric about the sub-earth point (numbered one to ten from the smallest) such that the area of each annulus was equal to its number times the area of the interior circle (the unit surface area). The projection of these segments onto the solar disk results in concentric circles with radii as indicated. The total number of data points within each annulus also appears. An examination of Table 1 makes obvious the fact that this approach over-samples portions near the center of the disk while near the limb the sampling rate declines drastically.

An attempt to temper the goal of equal area representation with the production of homogeneous means utilized an approach similar to the

Table 1. Sample distribution of data points within annular rings representing multiples of equal surface area.

<u>Ring No.</u>	<u>Ring Radius as Projected on Disk</u>	<u>No. Points/Unit Surface Area</u>
1	0.17	610
2	0.34	871
3	0.45	529
4	0.57	498
5	0.70	447
6	0.79	245
7	0.88	172
8	0.94	57
9	0.99	8
10	1.00	0

Table 2. Sample Distribution of Data Points Within Annular Rings
Representing Multiples of Equal Disk Area.

Ring No.	Radius on Disk	No. Points/Unit Disk Area	Area of Solar Surface Per Unit Disk Area	No. Points/0.01 Part Surface Area
1	0.134	380	0.0090	422
2	0.234	383	0.0095	403
3	0.330	354	0.0098	361
4	0.424	329	0.0100	329
5	0.523	318	0.0108	294
6	0.618	271	0.0111	244
7	0.717	243	0.0127	191
8	0.809	183	0.0135	135
9	0.904	129	0.0180	71
10	1.000	30	0.0430	7

previous one, namely dividing the solar disk into equal area segments. As Table 2 indicates the number of points per unit surface area declines more slowly as the limb is approached.

An additional attempt was made to lessen the decrease in the number of data points per unit surface by setting the widths of the annular rings equal. Comparable data for this configuration appear in Table 3. The term equivalent sector will be used to denote the basic subdivision of each annular ring, i.e., 1, 2, . . . 10. Unit area is no longer appropriate since the sectors are no longer of uniform size with respect to either the surface or disk. The fraction of the solar surface represented by each (equivalent) sector varies by a slightly larger amount than in the arrangement represented by Table 2. However, the number of data points per unit surface area decreases at a slightly slower rate in the vicinity of the middle rings.

The last method (see Figure 2) was adopted to preliminarily divide the data into sectors which when further subdivided into a given number of equal parts would produce homogeneous mean values. The remaining question to be explored concerns the further subdivision of these equivalent sectors to adequately remove the convective motions while attempting to retain any structure which may exist in the flow.

While performing the foregoing analysis, it was discovered that a systematic center to limb variation existed within the line-of-sight data. Figure 3 depicts the difference between adjacent annuli of the mean value

Table 3. Sample Distribution of Data Points Within Annular Rings of
Equal Width.

Ring No.	Radius on Disk	No. Points/Equiv- alent Sector	Surface Area/Equiv- alent Sector	No. Points/0.01 Part Surface Area
1	0.1	202	0.0050	404
2	0.2	323	0.0075	430
3	0.3	335	0.0087	385
4	0.4	332	0.0093	357
5	0.5	311	0.010	311
6	0.6	283	0.011	255
7	0.7	247	0.012	206
8	0.8	202	0.014	144
9	0.9	139	0.018	77
10	1.0	33	0.044	8

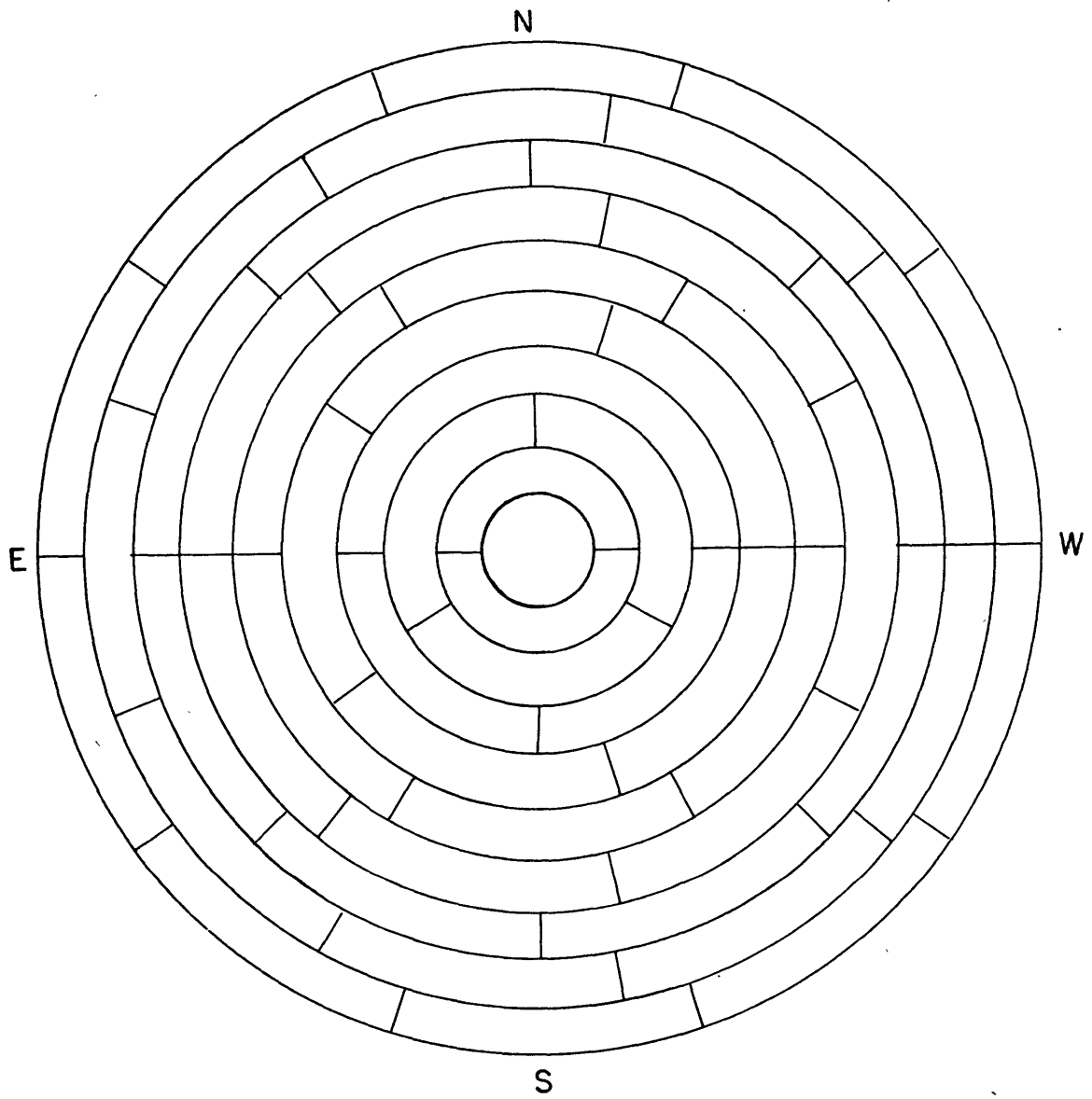


Figure 2. Distribution of equivalent sectors over the solar disk.

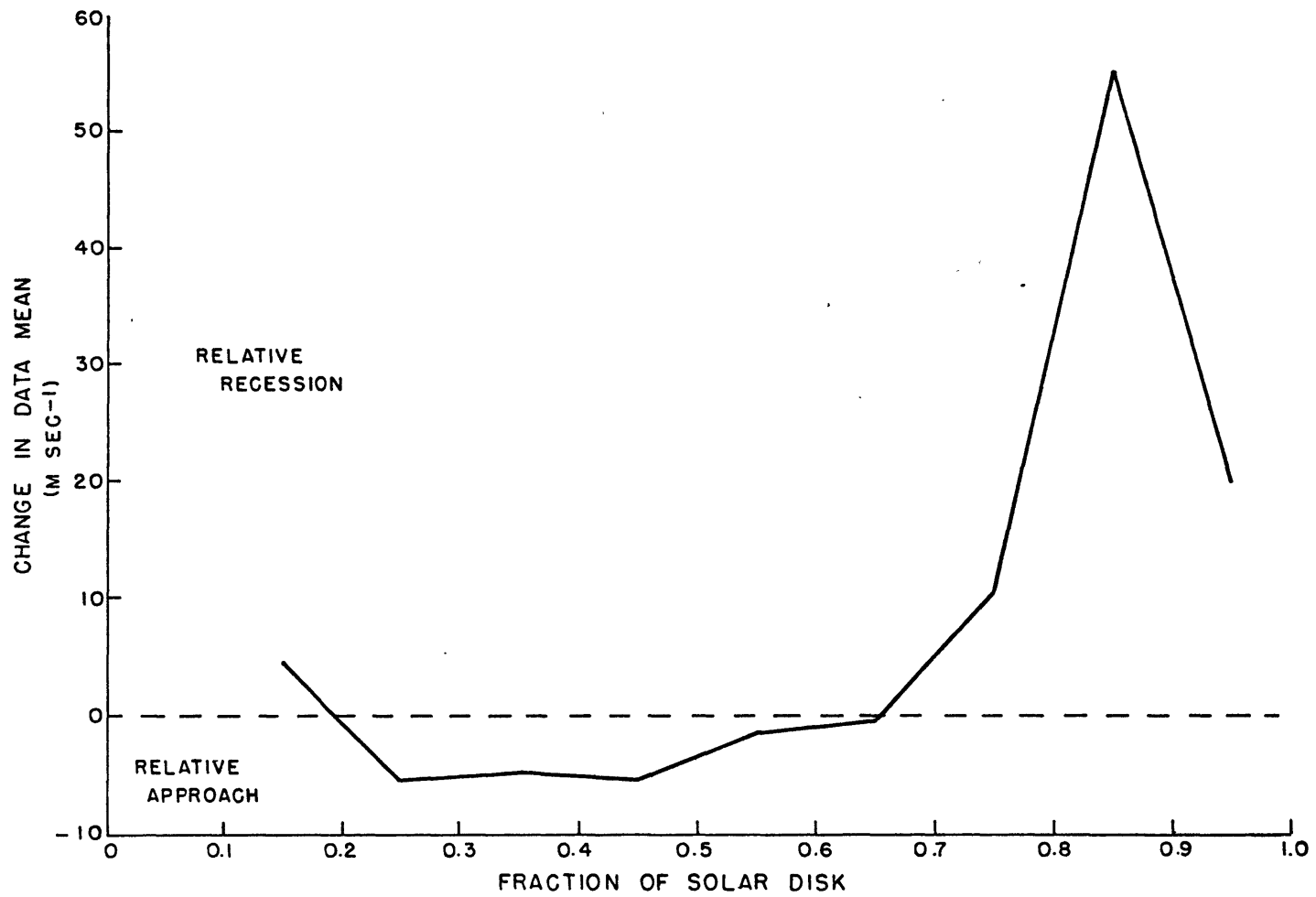


Figure 3. Center to limb variation in the mean Doppler velocity data determined for each annulus from all available measurements.

for the entire period of all points within the ten concentric circles. The pronounced increase in the mean line-of-sight velocity limbwards of 0.8 central distance indicates that on the average the limb is receding with respect to the remainder of the disk, clearly not a physical occurrence. There are similar trends near the center of the disk on certain days, most notably on 01, 09, and 14 July. However, since the center of the disk represents a continuous area, it is possible that there is some coherent motion in this area which results in a different value for this annulus average. This is almost certainly the case on 01 and 09 July when sunspots occur near the sub-earth point. (Howard observes predominantly downward motion over active regions.) However, in the case of the outer rings there is such a wide range of latitudes and longitudes represented that it is difficult to imagine a dynamic cause for a systematic recession of the outermost rings.

It is suggested that the limb reddening discussed previously contributes to this relative motion. The study by Hart may lead to a more precise accounting for this phenomenon which could reduce this systematic effect. Future improvements notwithstanding, it was decided to utilize only that portion of the data out to a central distance of 0.8. The data in these rings were normalized by subtracting the annulus average.

Having reached a decision on how best to represent the solar surface with the data at hand, it remains to determine how finely to divide each equivalent sector to eliminate unwanted effects. Since there is no way

a priori to decide when all the effects of convection and other random noise have been removed, establishing the size of this optimum area depends as much on the appearance of the final product as on the physical dimensions of the most prevalent convective mode. The preliminary streamfunction calculations necessary to resolve this question were accompanied by their own peculiar set of problems which required solution before any final judgments were possible.

3.3. Mechanics of the Analysis

According to Equation (5), the difference in the streamfunctions between any two points along the path of integration is the integral of the line-of-sight velocity along the path length connecting the points in question. In order to apply this result to the present study the corresponding finite-difference approximation to Equation (5)

$$\psi_{i+1} = \psi_i + \hat{V}_{l(i+1,i)} \Delta S \quad (14)$$

is used. The variables $\psi_{(i+1)}$ and ψ_i are the streamfunctions at successive points $i+1$ and i separated a distance ΔS measured along the arc over which a mean line-of-sight velocity \hat{V}_l is observed.

There is no stipulation contained within (5) which restricts the manner in which ΔS is defined. The result should hold whether ΔS is large or small and ought not depend on a regular spacing providing the mean value for V_l is a faithful representation of the actual distribution of V_l along ds . In the case under consideration, the foregoing analysis dealing with the most appropriate data averaging technique provides mean values

at regular intervals around each circle, the final spacing dependent on the number of subdivisions of the equivalent sector. Future results may suggest an advantage to be gained by nonuniform spacing between mean data points but none is apparent now and the present study will not consider such a case.

As mentioned, all streamfunctions are determined to an additive constant and the success of the procedure in producing a continuous field of values lies in being able to relate all streamfunctions to one common (but still unknown) constant. The absolute values are not necessary since the velocities are proportional to the streamfunction gradient.

As Gilman (1971) points out, one procedure which yields a continuous field of values (referred to in what follows as "closing" the technique) is the specification of the streamfunction along a curve which cuts all the integration paths. This immediately establishes a common reference for all paths, resolving the problem directly. Specifically, Gilman's suggestion that ψ_0 be set to zero along the equator (consistent with no flow across the equator) was adopted as a first try at closing the analysis technique. This specification was used by Fischer when testing the technique on terrestrial data. While his ultimate result compared favorably with the flow pattern analyzed directly, some adjustment was required to insure that ψ vanished identically when a semi-circular integration path (similar to that between points A and B in Figure 4) was traversed. The source of the residual was not readily apparent; possible contributions included inadequate representation of data due to a coarse grid, the small

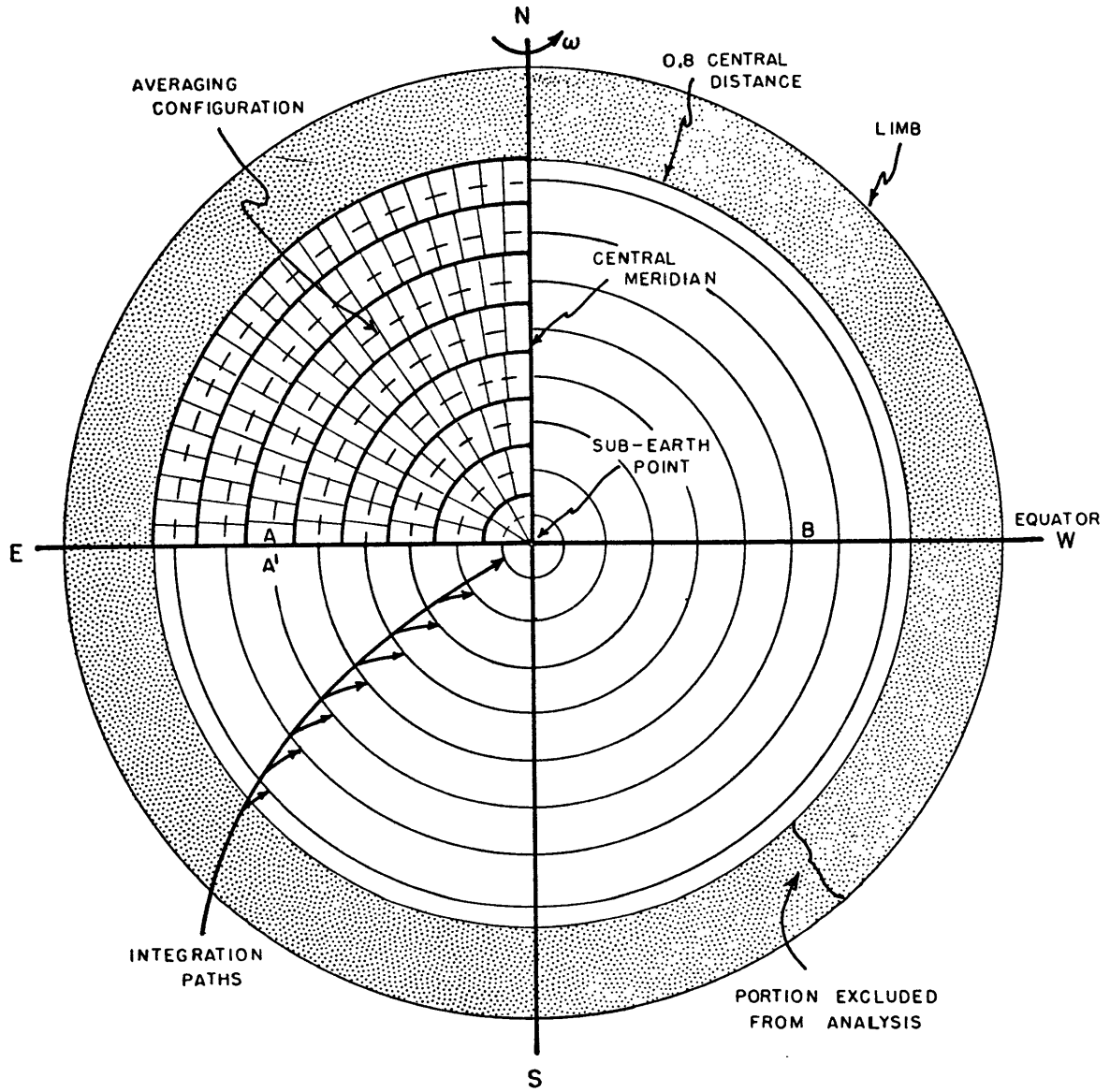


Figure 4. Final data averaging configuration and location of the integration paths.

cross-equator flow present in the sample and the divergence and vertical motions associated with convection. Since these processes have the potential for even greater impact on the outcome of the solar analysis, it was not entirely unexpected when the identical procedure proved to be inadequate in the trial run which follows.

A trial analysis was performed using the solar data with the equivalent sector divided arbitrarily into eight subdivisions. Since the streamfunctions were to be calculated beginning on the equator, the subdivisions were chosen to assure that no resulting data would lie directly on the equator. The calculations were performed beginning at the equator in the eastern (left) hemisphere and proceeded in a clockwise direction. Both choices, i. e., point of origin and direction, were arbitrary and as later comparison will show, other choices produced similar results.

A typical result of this analysis is contained in Table 4 which lists the values of the streamfunctions for the equator in the western and eastern hemispheres respectively as well as the maximum value of ψ calculated along each path. Recall that the calculation began in the eastern hemisphere with an assumed value of $\psi_0 = 0$, then proceeded in a clockwise direction. If the assumption that $\psi_0 = 0$ along the equator were essentially correct, the values tabulated in Table 4 should be in the vicinity of zero. Even allowing for imperfections in both technique and data, this is clearly not the case. It is immediately apparent that there is a discontinuity in the flow pattern at the equator resulting from the

Table 4. Values of the streamfunctions at the western and eastern hemisphere equators which result after completing half an integration path assuming $\psi_0 = 0$ on the equator.

<u>r</u>	<u>West</u>	<u>East</u>	<u> Max ψ </u>
0.05	103.2	-89.2	103.2
0.15	83.6	-87.2	87.2
0.25	8.4	-5.9	100.0
0.35	16.3	-21.8	164.9
0.45	21.3	-19.8	195.2
0.55	27.3	-32.0	217.7
0.65	50.2	-50.8	243.0
0.75	44.1	-42.8	236.7

assumed constancy of the streamfunction there (see Figure 5). The pattern in low latitudes for both hemispheres strongly suggests that flow occurs across the equator on the sun. Questions regarding the reality of such flows, or more generally of the entire pattern, will be set aside until a more realistic appearing result is obtained.

The qualitative assessment of these initial results suggest the form of the next attempt, but more positive justification can be found in an examination of the calculations performed along each integration path. Note that the sums of the streamfunctions at the equator in the western and eastern hemispheres contained in Table 4 are relatively close to zero suggesting that mass continuity would be maintained along the horizontal surface when the net flow across closed circular paths is considered.

As was the case when testing the technique using terrestrial data, the value obtained at the completion of the integration is not precisely equal to that assumed at the start. Comparison of each residual (the sum of Ψ on the equator in both hemispheres) with the maximum value encountered along each path gives an indication of their relative magnitude. With the sole exception of the innermost circle, the residuals represent less than 5 percent of the maximum value. The larger value associated with the innermost circle may be due to the presence of an active region in the vicinity of the sub-earth point on this particular day. A positive residual, if real, would indicate a net outflow of mass across the circle. This may very well be the case when an active region is enclosed since Howard (1971)

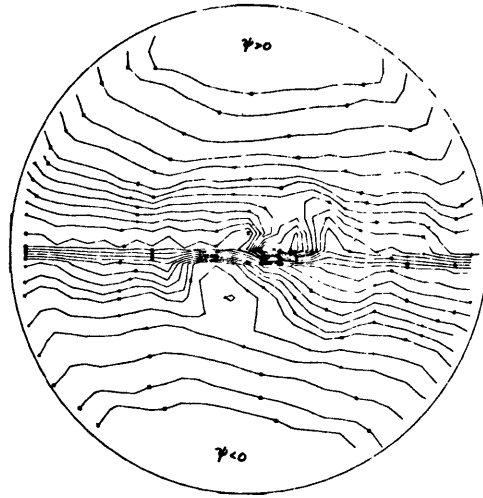


Figure 5. Sample flow pattern which results when ψ_0 is assumed to be zero along the equator.

observes a downward motion at this level in the vicinity of active regions. If such motions represent material descending from above, a net flow across a closed path could occur.

To avoid the discontinuities which these residuals would introduce into the flow patterns, the line-of-sight velocities were adjusted to eliminate net flows across the closed paths. This adjustment consisted of subtracting V_l^* from each mean line-of-sight velocity around the respective circle, where V_l^* the mean correction is defined as

$$V_l^* = \frac{1}{N} \sum_N (\hat{V}_l)_N \quad (15)$$

Generally, such corrections were quite minor, $\sim 5 \text{ m} - \text{sec}^{-1}$, although for the innermost circle in the example given $V_l^* \approx 30 \text{ m} - \text{sec}^{-1}$. Without exception the highest corrections occurred on the innermost circles where the component of horizontal velocities in the line-of-sight is small. Thus, the chance for contamination by spurious effects and net vertical motions is greatest.

Relaxation of the constraint prohibiting flow across the equator, while allowing calculation of continuous streamfunctions for each circle independently, leaves behind a more serious problem. There is no longer any a priori justification to specify the position of a streamline within the flow and, as a result, no direct relationship exists among the streamfunctions on each characteristic circle. It is mathematically correct to proceed as before, i.e., assuming $\Psi_0 = 0$ on the (eastern) equator, but the resulting flow field would contain a barrier across which no flow may

occur. Clearly, there is no physical justification for this result, requiring that an alternative approach be sought to close the technique.

A solution to this problem can be found within the original definition of the streamfunction. In heliographic coordinates the components of velocity in the meridional (Θ) and zonal (λ) directions are given in terms of the streamfunction, Ψ , by

$$V_{\lambda} = -\frac{\partial \Psi}{\partial \Theta} ; \quad V_{\Theta} = \frac{1}{\cos \Theta} \frac{\partial \Psi}{\partial \lambda} \quad (16)$$

If the heliographic coordinates are transformed into a new system, α and φ , where α is the azimuth angle about the sub-earth point and φ is the central angle, the velocity components in the α and φ directions can be obtained (see Appendix A):

$$V_{\varphi} = r^2 \frac{\partial \Psi}{\partial \alpha} ; \quad V_{\alpha} = -\frac{\partial \Psi}{\partial \varphi} \quad (17)$$

Since $ds = r d\alpha$ and $V_{\alpha} = r V_{\varphi}$, the relationship defining is the differential form of Equation (5) from which the streamfunctions were originally defined. It follows then if V_{α} could be determined along paths of constant α , the variation of Ψ with φ would be specified and a continuous field of Ψ for the entire disk produced. Unfortunately, V_{α} is everywhere perpendicular to the line-of-sight and is undetectable making a point by point determination of $\partial \Psi / \partial \varphi$ impossible.

However, it is possible to arrive at a closure method (albeit a less restrictive one) by considering the ensemble of streamfunctions along each path.

If radial differences in streamfunctions are representative of the velocities in the azimuthal direction on a point by point basis, the sum of these differences around adjacent circular paths must be proportional to the net velocity within the annulus. The sum of these tangential velocity components represents the circulation C in the annulus

$$C = \oint_s V_\alpha(s) ds \quad (18)$$

If the tangential velocities are uniformly distributed along ds , then

$$C = V_\alpha \oint_s ds = 2\pi r V_\alpha \quad (19)$$

for the situation under consideration.

A mean tangential velocity for each annulus can be defined such that

$$V_\alpha^* = \frac{1}{N} \sum_N (V_\alpha)_N \quad (20)$$

The circulation around the annulus then becomes

$$C = 2\pi r V_\alpha^* \quad (21)$$

and by virtue of the definition of V_α and its average

$$C \propto \left(\frac{\partial\psi}{\partial\varphi}\right)^* \propto \frac{\partial\psi^*}{\partial\varphi} \quad (22)$$

Recalling that the annular rings are all defined with respect to the sub-earth point and that the location of this point is determined by the sun-earth geometry and always lies within $\pm 7^\circ$ of heliographic latitude of

the solar equator, the assumption is made that no net circulation exists about the sub-earth point. In light of the high zonality of the flow within the solar atmosphere, this assumption would appear to be a valid one. It would be difficult to imagine flow patterns existing which would produce an appreciable circulation in the outermost annuli which include the higher latitudes of both hemispheres as well as widely separated segments in the equatorial regions. It would not be difficult on the other hand to have real circulations completely enclosed by the smallest circular paths.

From the assumption that no net circulations exist in the annuli it follows that the mean values of the streamfunctions for each path of integration be equal. It should be recognized that while this assumption might be completely valid for flow in the solar photosphere, establishing such a relationship among the various mean values of the streamfunctions will result in an azimuthal smoothing of the resulting patterns.

The foregoing analysis is strictly correct only when the sub-earth point lies directly on the solar equator ($B_0 \equiv 0^\circ$). For other positions, a small, but real, circulation will be present in the annular rings. This circulation is due to the component ($\propto \sin B_0$) of the solar rotation axis which is enclosed by the annular rings. Since all velocities have been defined relative to the solid body rotation at $\pm 20^\circ$ latitude (based on Howard's long term mean profile), this circulation must be defined likewise. A more exact determination would result if the daily profile was used since appreciable excursions from the mean have been observed.

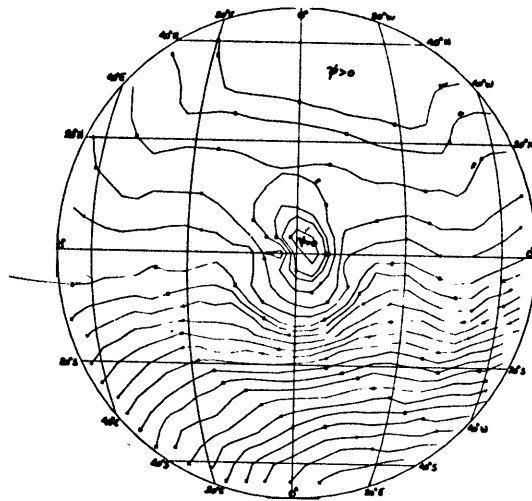
However, since B_o is limited to values between -7° , the overall differences are small and it was deemed adequate for the present purpose to base this correction on the mean differential rotation profile. The mean velocity component around each annulus was calculated and the corresponding difference in the average streamfunctions determined for the range of B_o (see Appendix B). The results appear in Table 5. Since the tangential velocity between any two points is otherwise determined by a constraint on the average velocity around each annulus, no attempt was made to reproduce the actual tangential velocity distribution due to this effect even though it was known. Denoting the difference between the mean streamfunction on a given circle and the mean chosen as the reference as $\Delta \psi^*$, individual streamfunctions were adjusted in the following manner:

$$\psi_{\text{CORR}} = \psi_{\text{CALC}} + \Delta \psi^* \quad (23)$$

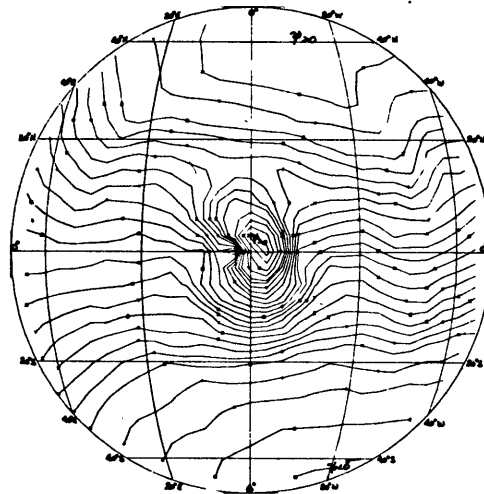
This closure procedure ought not to be dependent on the integration path used as the reference. Only the numerical value of the streamfunction at a given point will depend on the reference. However, since only gradients of the streamfunction are involved, the results should be comparable. Verification of this contention was made by comparing the patterns produced using as references the innermost ($r = 0.05$) and outermost ($r = 0.75$) circles respectively. These results appear in Figure 6. A first glance gives the impression that the result based on the outermost circle contains more intense gradients. Such is not really the case; the

Table 5. Change in the value of ψ^* on successive integration paths corresponding to the mean net circulation observed in each annulus when $B_0 \neq 0$. The values of $\Delta\psi^*$ are negative (positive) for positive (negative) values of B_0 .

B_0	<u>Interior Ring Number</u>								
	1	2	3	4	5	6	7	8	9
7	0.3	0.6	1.0	1.4	1.9	2.3	2.6	2.7	2.2
6	0.3	0.6	0.9	1.2	1.6	2.0	2.3	2.4	1.9
5	0.2	0.5	0.7	1.0	1.3	1.6	1.9	2.0	1.6
4	0.2	0.4	0.6	0.8	1.1	1.3	1.5	1.6	1.3
3	0.1	0.3	0.4	0.6	0.8	1.0	1.1	1.2	1.0
2	0.1	0.2	0.3	0.4	0.5	0.7	0.8	0.8	0.7
1	0.0	0.1	0.1	0.2	0.3	0.3	0.4	0.4	0.3



Innermost path



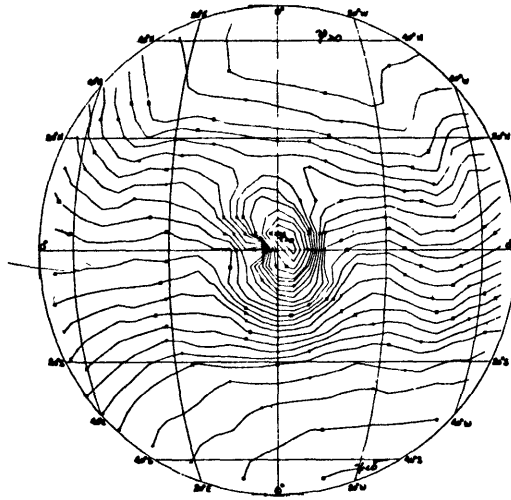
Outermost path

Figure 6. Comparison of the flow patterns obtained when selecting ψ^* from the innermost and outermost integration paths.

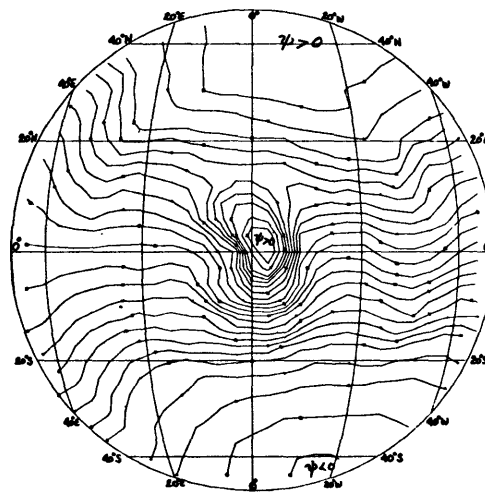
apparent discrepancy is due to the selection of non-uniform intervals between isopleths which increase as the absolute magnitude of the streamfunction increases. Thus, a pattern which contains streamfunction values more uniformly distributed around zero will have more isopleths drawn than one with a more asymmetrical distribution. In the case illustrated, the result based on the innermost circle produced streamfunctions ranging in value from -80 to 280 while the outermost circle produced a range from -180 to 180. This disparate effect is most pronounced in the vicinity of the maximum located near the sub-earth point. It was decided to reference the streamfunctions to the innermost integration path.

The effect of starting the integration at the equator in the eastern hemisphere was also considered. Here again it seemed unlikely that any differences should result once the mean data were obtained since the streamfunctions would be dependent on the same paths and data regardless of the point of origin for the calculations. This assumption was tested by comparing the patterns in their present form with their counterparts obtained by beginning at the equator in the western hemisphere and integrating in a counter-clockwise direction. The results (Figure 7) are nearly identical with the minor differences attributable as before to differences in streamfunction magnitude and isopleth intervals.

This technique has now evolved to the point where only the size of the averaging area need be specified before a series of daily flow patterns can be produced. As has been already stated, convection is a fundamental



Origin in eastern hemisphere



Origin in western hemisphere

Figure 7. Comparison of the flow patterns obtained from stream-function calculations starting on the equator in the eastern and western hemisphere.

process in the solar atmosphere and the entire procedure outlined thus far is highly dependent on the assumption that in the layer being sampled motions are primarily two-dimensional and nondivergent. It has been demonstrated that this layer lies above the main convective zone although its lowest depths are probably influenced by the underlying convection. Since the photosphere is generally assumed to be a free surface across which no material flows on the average, contributions to the line-of-sight velocity data due to vertical motions can be minimized if the data are averaged over an area larger than the basic convective scale size.

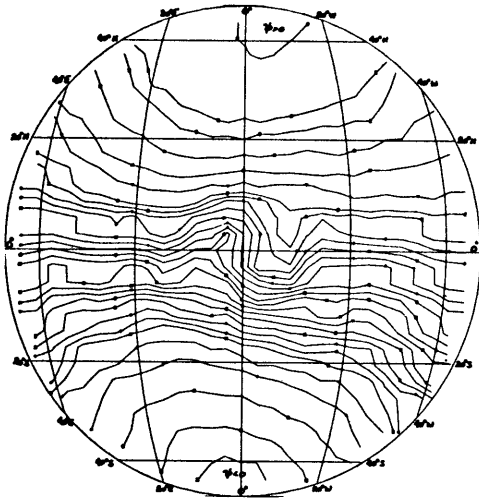
Observations have established that convection in the solar atmosphere occurs on two characteristic scales, the granulation 10^3 km in diameter and the supergranulation two orders of magnitude larger. The vertical motions associated with the granulation are generally an order of magnitude greater than those within the supergranulation, the former probably results from instabilities within a shallow layer at the top of the convective layer while the supergranulation may extend to depths approaching 10-15 per cent of the solar radius.

If the contribution from these vertical motions are to be effectively removed from the line-of-sight velocity data, the averaging must range over an area sufficiently large to include a few supergranules. Satisfying this condition will assure adequate representation of the smaller scale granulations as well as reducing the contributions from the vertical motions associated with this convective scale.

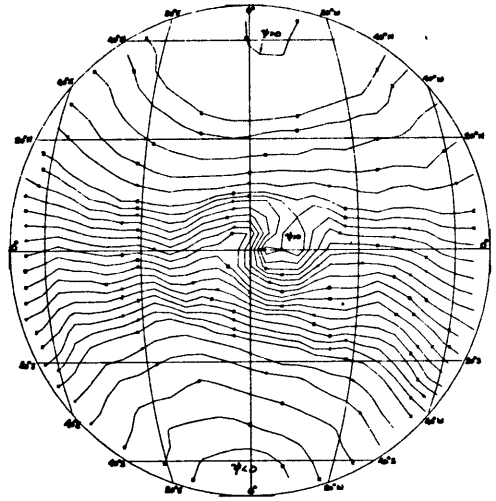
Based on the statistics describing the supergranulation (Simon and Leighton, 1964) a typical diameter is 3×10^5 km and approximately 2500 cells are present on the visible hemisphere at a given time. The mean lifetime is on the order of 20 hours suggesting that ~ 90 percent of the total are present in whole or in part for the period of time (1 1/2 hours) required to complete the measurements for the entire disk.

Table 3 lists the fraction of the surface area which each primary equivalent sector represents. On the average each equivalent sector represents one percent of the surface area. If there are 2500 supergranules on the visible hemisphere at a given time, each equivalent sector includes roughly 25 supergranules. At a maximum the equivalent sector was divided into twelfths ($N = 12$) to include data from an area generally equivalent to two supergranules. For comparison, the analysis was performed on mean data based on quarters ($N = 4$) and eighths ($N = 8$) of the equivalent sector to judge the overall effects of differing resolutions as well as the tendency to average data over areas approaching the size of a single supergranule; a situation which occurs near the disk center in the $N = 12$ case.

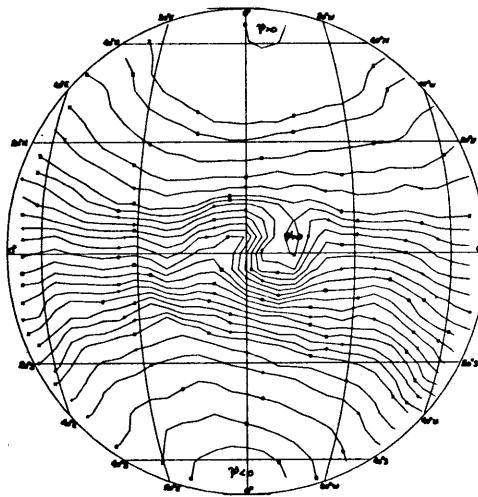
Figure 8 depicts the results of the varying resolution which upon inspection contains very few real differences. The jaggedness in the isopleths for the $N = 4$ case is due to the linear interpolation technique which the contouring program employed. As the number of data points increased, the contours become smoother. From the standpoint of the flow, however,



N = 4



N = 8



N = 12

Figure 8. Comparison of the flow patterns obtained from equivalent sectors divided into 4, 8 and 12 equal parts prior to averaging.

the grosser the averaging the smoother the resultant flow pattern, the expected result. The differences in pattern smoothness are rather subtle over the range of averaging areas represented and are most readily apparent when comparing the trough-like feature near the center in the two extreme cases. The flow tends to have a smaller meridional component in the $N = 4$ case and the local range in values of Ψ is likewise smaller. A judgment as to whether this slight difference is due entirely to the size of the averaging area, the tendency to resolve single supergranules towards the disk center or a combination of both, must be deferred until more experience in interpreting the results is accumulated. Nonetheless, since there were no appreciable differences among the three resolutions investigated, the first ($N = 12$) was chosen for use since it had the potential to retain the greatest detail.

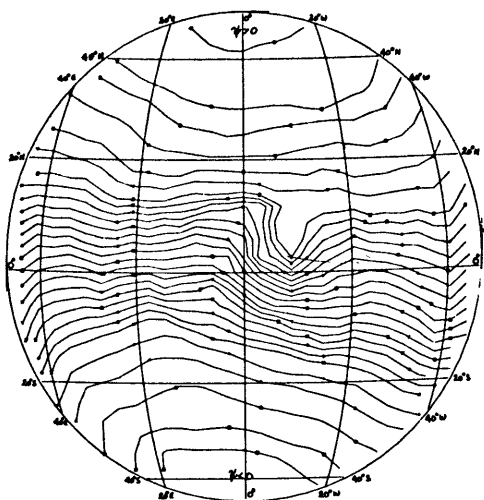
Based on the foregoing series of experiments, the technique was judged to be in a form which would produce the most favorable results. These results, their validation and implications occupy the remainder of this work.

4. How Well Does the Technique Work?

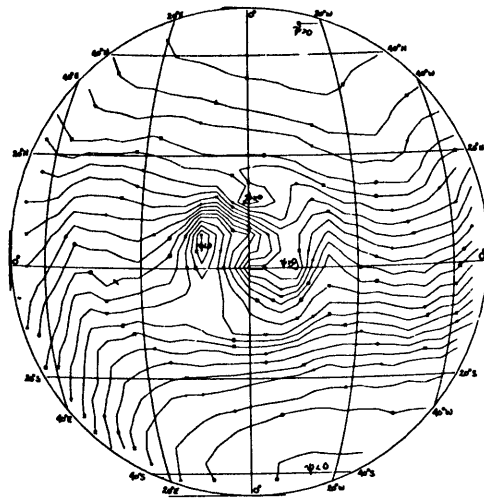
Up to this point in the technique development, the main consideration has been the production of flow patterns which are physically realistic, i.e., contain no discontinuities, artificial barriers, etc., while simultaneously attempting to insure that the final version was independent of the technique. Judging each daily result individually, it appears that flow patterns which conceivably could serve as realistic characterizations of the flow in the solar atmosphere have been produced. However, as was pointed out in the introduction, the sun exhibits a degree of continuity when other solar phenomena are observed, and a similar continuity should be expected when considering the flow field as well. Perhaps the combined natures of the observations and technique will allow at present only a topological representation of the flow actually existing at this level in the solar photosphere. Nonetheless, some verification must be accomplished before the technique can be considered valid to any extent.

4.1. A Qualitative Assessment

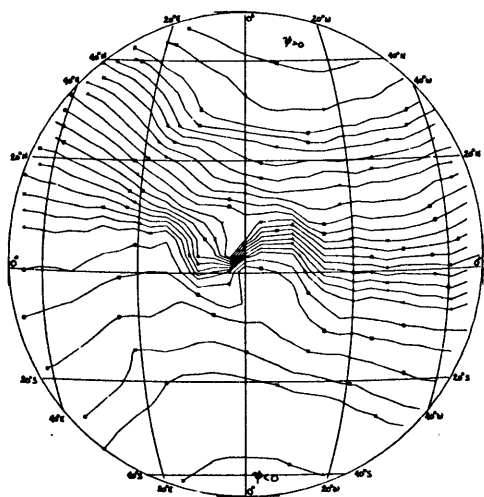
Flow patterns inferred from the Doppler measurements made during the period 30 June - 14 July 1972 inclusive (07 July missing) appear in Figure 9. Since extra time and effort are required on the part of Mt. Wilson Observatory personnel to provide the data in a form amenable to the present use, this two week data represents the entire sample acquired. It is readily apparent that the potential knowledge to be gained from the analysis described here will be realized only after large amounts of data representing



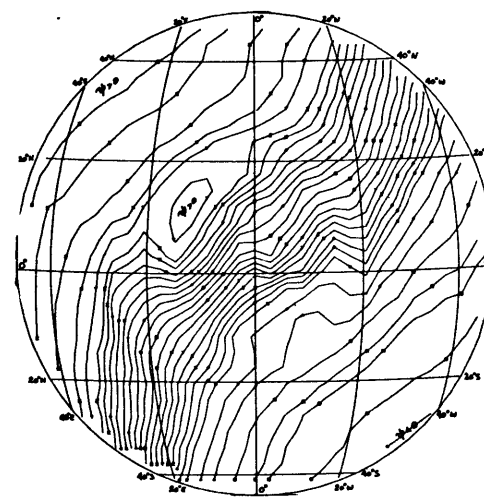
30 June



01 July

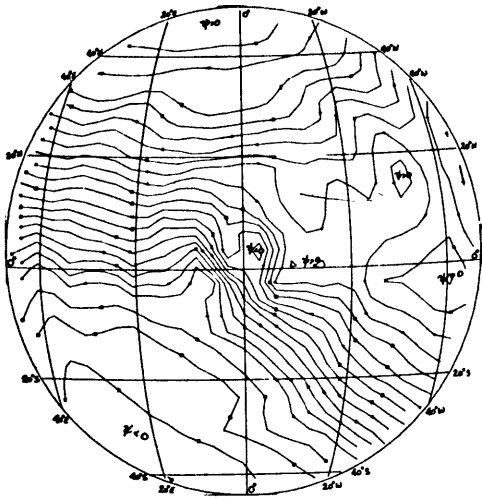


02 July

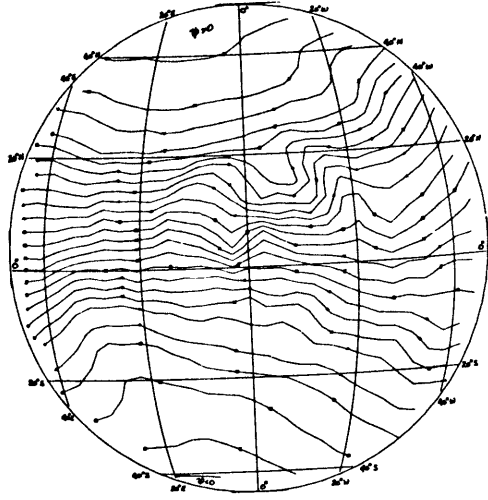


03 July

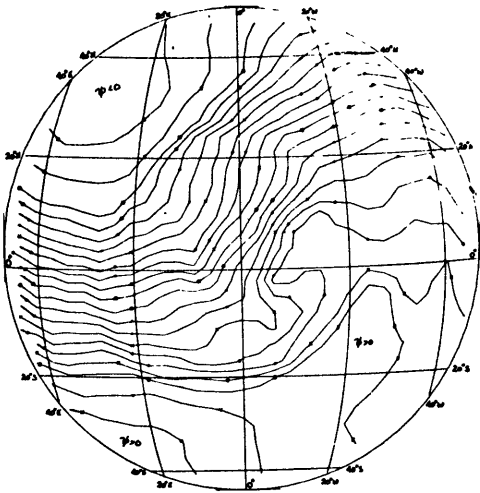
Figure 9. Final version of the flow patterns for the period 30 June - 14 July 1972.



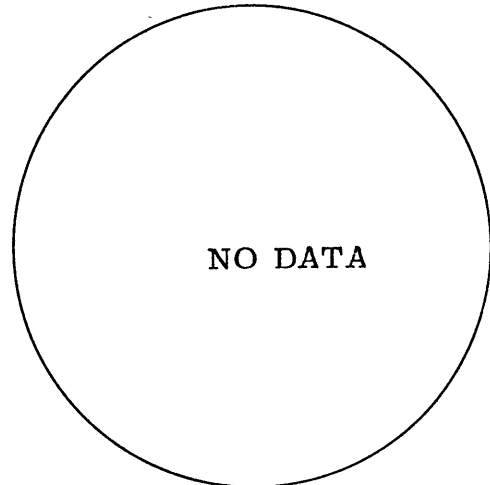
04 July



05 July

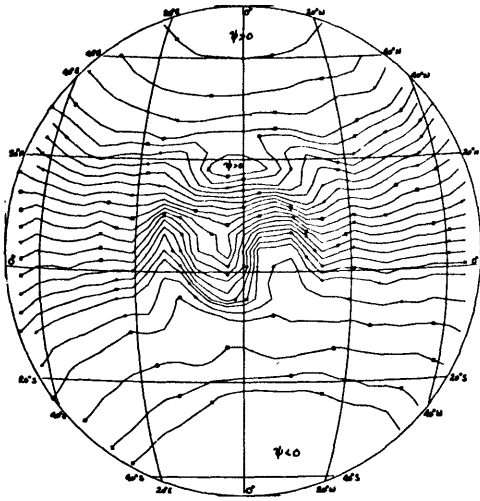


06 July

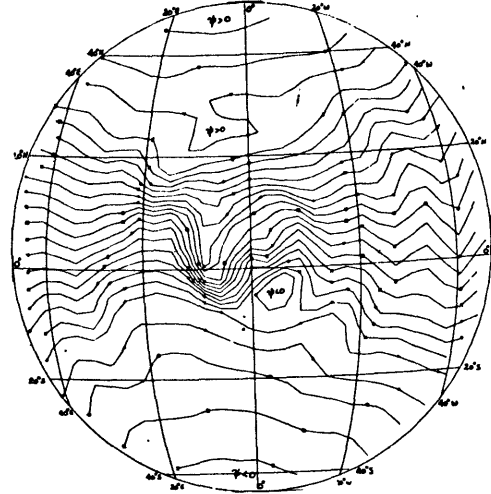


07 July

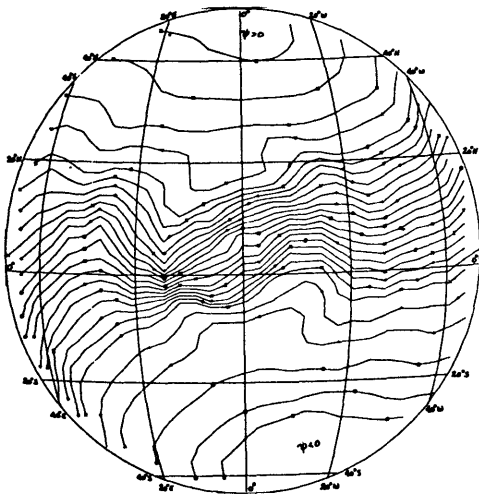
Figure 9. (continued)



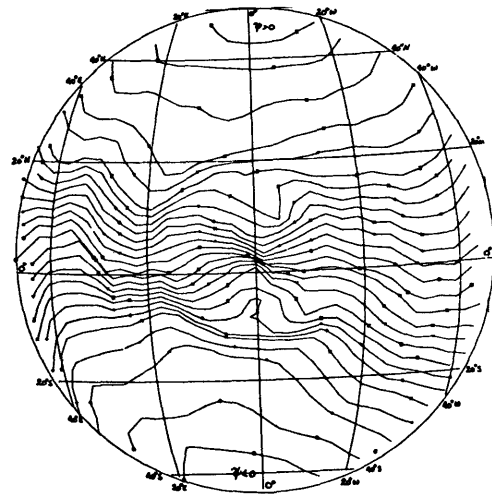
08 July



09 July

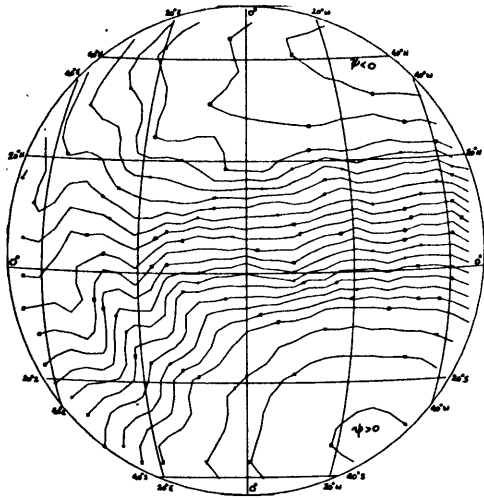


10 July

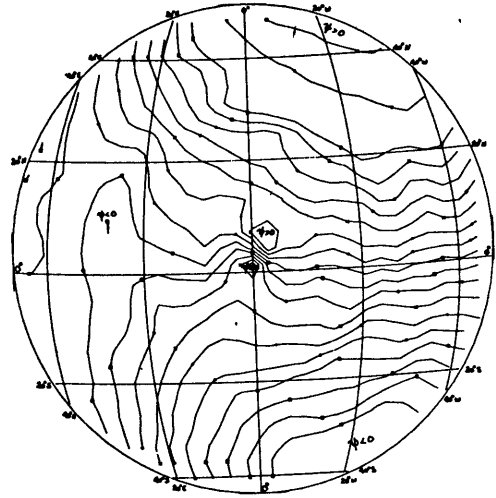


11 July

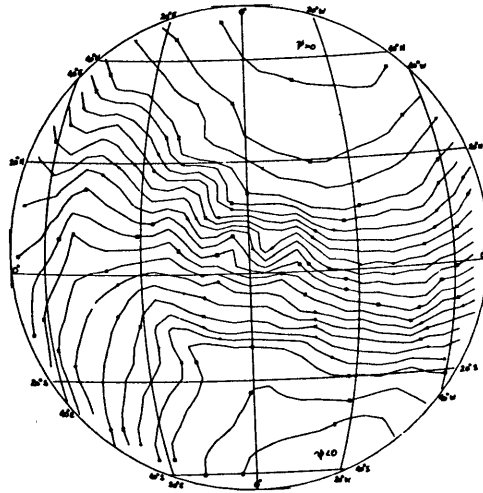
Figure 9. (continued)



12 July



13 July



14 July

Figure 9. (continued)

various phases of the solar cycle have been similarly processed. Since, however, the current effort is directed primarily at developing the analysis technique, it was decided to require that some degree of success be demonstrated using a modest amount of data prior to requesting a more extensive sample.

The patterns in Figure 9 are presented for consideration as the initial representation of the flow field occurring in the solar photosphere during the time of observation. The sub-earth point is located at the center and the rim of the circle represents a central distance equal to 0.75 , the locus of sector centers of gravity in the largest annulus used. In terms of heliographic coordinates, coverage is generally complete between $+40^\circ$ latitude and $+40^\circ$ central meridian distance and extends to portions of latitudes and central meridian distances near $+50^\circ$. The asymmetric extent in latitude reflects the non-zero value for the latitude of the sub-earth point (B_0) which ranged from 2.90° to 4.35° during the period. Finally, recall that the flow has been defined with respect to an underlying solid body rotation (left to right) equivalent to the long-term mean Doppler determined rate at $+20^\circ$ latitude, and there is only a relative relationship among the streamfunctions and their gradients for any combination of days.

Most obvious when examining the patterns for this period is the meandering nature of the flow. There is little tendency for strict zonality although it is readily apparent that a larger zonal than meridional component does exist, the pattern for 03 July (about which more will be said

momentarily) excepted. It is interesting to note that these deviations from zonality are not randomly oriented in space, but appear to be organized on a large scale producing patterns which bear a resemblance to flow structure observed to occur in the earth's atmosphere. Specifically, there appear to be closed circulation centers poleward of $+40^{\circ}$ latitude which persist and exhibit a general left to right motion across the disk. The day to day progression of these features, if stationary with respect to the underlying solid body rotation, is not in strict accord with that rotation rate ($\sim 14^{\circ}$ CMD - day⁻¹). However, if the period from 04 - 14 July is taken as an example of the interval for the semi-closed circulation centers in both hemispheres to move across the portion of the disk pictured, a rough correspondence does exist. The discrepancy is most likely smaller than these results indicate since the combined effects of geometrical foreshortening and data averaging tend to displace the position of these features towards the central meridian giving the appearance of a slower movement than might actually exist. Furthermore, if these features were subject to Rossby-wave dynamics, their motion would be retrograde with respect to the underlying solid body rotation at approximately 1° per day based on wave number 4 or 5 as suggested by some of the patterns (e.g., 06 July).

The pattern for 03 July differs markedly from the others and appears to be the result of a misorientation. If it were rotated 90° clockwise, a fair degree of continuity would result for the three day period 02 - 04 July

including the position and rotational motion of the closed feature in the (then) western half of the northern hemisphere. Unfortunately, there was no justification for such an adjustment -- a check with Mt. Wilson personnel was unable to confirm or deny any misorientation. Regardless, the pattern on this day was not considered in the investigations which follow.

On two occasions, 01-02 July and 08-09 July, small-scale waves appear in the vicinity of the sub-earth point. These features are located in close proximity to sunspots which may actually distort the large-scale flow. However, there may also be a spurious contribution to this distortion from the general downward motion observed to occur in the vicinity of active regions. Such motions, if organized on a larger scale than that considered when spatially averaging the data, would introduce an additional spurious component into the horizontal streamfunctions. This component would be most intense near the sub-earth point where the chance for contamination is greatest since smaller surface areas are represented by each mean data point and real horizontal motions contribute small components to the line-of-sight velocities. The distortion in the flow pattern near the center on 13 July is not associated with an active region and is most likely due to a defect in the data and/or analysis.

The measurements for two days 06 and 12 July indicate that the entire portion of the disk represented has a mean rotation slower than the reference rate. The patterns on these days contain relative easterlies rather than the westerlies which exist in the mean and on most other days.

Such variations, if real, would appear to require sizeable transports of angular momentum out of low latitudes immediately preceding such an observation. This question will be explored more fully when discussing the implications of these results on the overall general circulation energetics.

Qualitatively, the results of this analysis show some tendencies toward reproducing flow patterns which bear similarities to analogous flows observed to occur in other rotating regimes. It might be tempting at this point to conclude that since the patterns were derived from solar observations and resemble flows seen in other rotating fluid regimes, these flow patterns must be representative of the actual large-scale flow in the solar photosphere. However, before any conclusion is reached, comparisons with other solar observations will be considered.

4.2. A Quantitative Judgment

Heretofore, the results of the various experiments have been judged primarily subjectively, attempting to reduce the effects of the small-scale vertical motions while maintaining in the final product as much structure as possible. Ideally, such choices should be based on a comparison of like quantities, one derived from the analysis being considered, the other obtained by a well established procedure. This path was available to Fischer when testing a similar streamfunction determination procedure on terrestrial data. Not only were the direct measurements available to produce flow patterns for comparison, but the assumptions upon which the technique is based are generally appropriate. Neither comparably

reliable alternative velocity measurements nor forehand assurance concerning the validity of the assumptions are available in the solar case.

However, while there are no independently obtained measurements of instantaneous velocities within the layer being sampled, there are daily observations of features at levels in the atmosphere which are close by in the vertical. If, as has been asserted in the introduction, there is a link between the dynamics of this layer and the overall general circulation energetics, there ought to be some correspondence of the large-scale flow in layers which are in close proximity. With this in mind, observations of other solar features were examined to determine how best to deduce the instantaneous spatial distribution of motions in the solar photosphere.

A question arises concerning the rationale behind the overall approach to the validation of the technique. If a quantitative assessment is possible now, why not introduce it at an earlier stage in the technique development and select the procedure which results in the best overall agreement suitably defined? Without a doubt, this approach is a more desirable one. However, it requires dividing the data sample available into two portions, one for the initial development and one to serve as an independent test. A sufficient amount of data is not presently available to use this approach. Additionally, the independent velocity measurements are derived from the day to day positions of features which do not reside at the same level represented by the Doppler velocity measurements.

It does not seem desirable to judge the best representation of the

flow at one level solely on measurements applicable to another level.

Finally, the nature of the features from which independent velocities will be derived is such that they tend to occur as part of active regions. As has been mentioned, the technique for producing horizontal flow patterns may not perform well in just these areas. If the final version of the technique was to be based on maximum agreement with the motions of these features, the overall results would be biased towards the portion of the flow field for which the analysis procedure is least applicable. Therefore, while the approach utilized to produce the final version of the flow patterns may not be optimum, it is free from these disadvantages. If it can be demonstrated that the patterns in their present form agree to some extent with other measurements with these shortcomings, might not it be likely that the patterns in other areas free from these disruptive features reproduce the actual flow even more faithfully? No doubt the experience gained from future more exhaustive comparisons with patterns obtained over a longer period than available here should result in a still better product.

A consideration of all solar observations which provide daily locations of distinct features and are made on a regular basis identified two potential candidates, calcium plages and sunspots, as independent measurers of velocities in the solar atmosphere. Neither is located wholly within the layer sampled by the Doppler line-of-sight measurements, the calcium plages residing in the less dense lower chromosphere ($\tau \sim 0.004$) while the sunspots are lower in the photosphere at the top of the convection

zone ($\tau \sim 1$). Both features have been used in the past to determine the mean rotation rate of their respective layers neither of which agrees with the Doppler derived rate or with each other. If the long term means do not agree, one can only wonder about daily differences. For various reasons plages are inadequate sources from which to estimate instantaneous velocity fields and will not be considered for this purpose.

Sunspots are well defined features occurring in the solar photosphere which have been carefully observed and their positions measured for nearly a century by the Royal Greenwich Observatory. Their positions are obtained from white light photographs of the solar disk and are determined to the nearest tenth of a degree. The center of gravity of a sunspot group can be located fairly precisely since sunspots have a fairly well defined boundary, are of smaller size and generally more regular in shape. The Greenwich sunspot observing procedure is part of a carefully controlled program and has produced a long series of homogeneous data and provides the most reliable source from which local velocity fields can be independently estimated.

The degree to which the velocities estimated from daily sunspot proper motions will agree with comparable velocities inferred from the Doppler measurements will depend as much on the performance of the sunspots as accurate tracers of the flow as it will on the validity of the patterns produced by the technique under test. Ward's studies previously mentioned which used sunspot motions to determine the mean rotation

rate have already shown that spot groups of different size and configurations yield different mean rotation rates. This suggests that not all spot groups trace the flow field equally well; at certain stages in their development their motion is dependent on other factors besides the bulk motion of the fluid in which they are imbedded. Magnetic field development or a dynamic interaction with their environment are just two examples of other factors which may influence the degree to which the spot group serves as an accurate tracer.

Nor is this the only shortcoming which is encountered when attempting to estimate local velocity fields in the solar photosphere from daily sunspot displacements. In order to get a representative sample of velocities, the tracers should be randomly positioned with respect to the flow. The deficiencies of spot groups when considering this requirement are twofold, not only are the spots generally limited to the portion of the solar surface between $\pm 30^\circ$ latitude, but they are located in a portion of the flow field which is different by virtue of the presence of the spot itself. Recall that there is already some indication that patterns inferred from the Doppler line-of-sight measurements may be of lesser quality in the vicinity of active regions.

Two potential contributions to the daily proper motions of sunspot groups exist which are not due to the motions of the surrounding fluid. One is the shift (in longitude primarily) of the center of gravity due to the geometrical foreshortening when the group approaches the limb. The

foreshortening tends to introduce a bias in the position in favor of the center of the disk. The other contribution is related to the average development of a sunspot group. Typically, the leader spot forms first and the center of gravity is defined accordingly. As the group evolves, the follower spot forms behind (on the east limb side) of the leader causing an eastward shift in the center of gravity of the group which is completely unrelated to any motions within the surrounding fluid. As the spot group evolves, further development and accompanying shifts in the center of gravity generally occur preferentially along a line connecting the leader and follower spots. The entire process is reversed during the decay of the group, the center of gravity progressively moves closer towards the leader spot, the last to disappear. These two motion independent contributions to daily proper motions of sunspot groups result primarily in spurious east-west motions. All things considered, the latitude of a sunspot group is more reliably determined than the longitude.

A more serious discrepancy may exist when attempting to use local fluid velocities derived from sunspot motions as a means to judge the validity of the flow patterns inferred from Doppler data. A recent study by Starr, Hendl and Ward (1974) shows that the covariance between the meridional and zonal components of sunspot proper motions when only fast moving spot groups are considered increases markedly over that obtained for the total spot population. The effect is observed for all sizes of sunspots but is most pronounced for the smallest category. Previous studies by

Ward (1964, 1965a) have been conducted using all but this subpopulation of sunspots with large motions which he attributed to errors in identification and measurement. Ward concluded that the sample he used ought to represent on the average any fluid motions organized on a large scale and his results tended to support such an assertion.

However, the more recent study by Starr, Hendl and Ward provides a more complete understanding of the reaction of sunspots to other scales of motion which exist in the surrounding fluid. Starr (1974) interprets the increased covariances obtained for the fastest moving spots in the following way. The increase in covariance for the fastest moving spots cannot be due to random errors since these would not be positively correlated. The magnitude of the increase (double in some cases) must be due to the existence of higher velocities than are attributed to the large-scale flow. Starr suggests that these fastest moving spots are responding more to the flow associated with the smaller scale convection. To support this contention he notes that the increase in covariance is greatest for the sunspots with areas ≤ 30 millionths of the visible hemisphere and is only slightly increased for the larger ones which at times approach the size of a typical supergranule. If this view is correct, observed sunspot motions are then the result of a variable response on the part of the sunspot to the motions associated with convection on one scale (supergranulation?) both of which are imbedded in and responding to flow organized on still a larger scale. Accordingly, smaller rapidly moving spots are most

affected by the convection while large slowly moving ones are more faithful tracers of the large-scale motions.

Clearly, such a situation poses a dilemma when attempting to validate flow patterns which are tailored to represent the flow on a large scale. The deficiencies inherent in sunspots as tracers of the ambient fluid are many and there is no way to estimate their overall reliability let alone even considering how to selectively choose the best of the lot. However, faced with the reality that no better source of solar data suitable for this purpose exists, a comparison of the velocities derived from daily proper motions of sunspot groups and those obtained from the flow patterns inferred from Doppler measurements will be made, keeping foremost in mind the deficiencies which exist in both.

4.2.1. Estimating Ambient Velocity Fields From Sunspot Motions

As mentioned above, it is not possible to correct for the deficiencies which undoubtedly exist when using sunspots as tracers of the surrounding flow field. It will be assumed, therefore, that the daily proper motion represented by the difference in sunspot group position on successive days is due solely to the large-scale motions of the fluid in which the group is imbedded. Under these conditions, the difference in sunspot group position on two occasions as determined by Royal Greenwich Observatory reflects the average fluid motions in the spot's vicinity in the interval between the observations.

Since the latitude of the center of gravity can be determined more precisely than the longitude for reasons already given, one source of uncertainty can be minimized if only the meridional components of the velocities are compared. This component is computed directly from the sunspot records by noting the change in the latitude of the group center of gravity from day to day. Daily changes on occasion exceed 2 degrees of heliographic latitude per day ($1 \text{ degree} - \text{day}^{-1} \approx 100 \text{ m} - \text{sec}^{-1}$).

Sunspot observations for the period corresponding to the flow patterns were obtained from Royal Greenwich Observatory. The day to day change in the latitude of each spot group located within 0.75 central distance was calculated and then used to represent the velocity in the vicinity of the sunspot on the earlier day. For example, if a sunspot group was located at 15°N on 30 June and 15.2°N on 01 July a velocity equivalent to -0.2° latitude per day (roughly $20 \text{ m} - \text{sec}^{-1}$) was assumed to be the meridional velocity component at the location of the sunspot at the time of the Doppler measurements on 30 June. The potential for error when using this mean velocity to approximate the instantaneous velocity is obvious. The negative (positive) sign which appears in the example indicates poleward (equatorward) motion; this sign convention is common to both hemispheres. The series of sunspot group observations used to perform the velocity estimates appears in Appendix C.

4.2.2. Estimating Velocity Fields from Streamfunction Patterns

In order to complete the comparison of the velocities derived from the two techniques, a method was developed to obtain comparable velocities from the streamfunction patterns. Recalling that the Doppler line-of-sight velocities are relative, the direct application of Equation (2) would result in horizontal velocity components which are relative as well. A means to equate the relative velocities calculated from the daily streamfunction patterns to actual velocities with respect to the underlying solid body rotation rate was necessary.

As best as could be determined, there was only one potentially successful approach to this problem -- the daily quantity determined from the greatest amount of data, the mean rotation rate, had to be used. The mean zonal velocity component relative to that at -20° latitude calculated from this rotation rate represents a constraint on all the individual values along each latitude on that day. Equation (2) can be applied to normalize on a daily basis the mean meridional streamfunction gradient for each latitude to its respective value of mean (relative) zonal velocity. The procedure is as follows; the mean (relative) zonal velocity V_{λ} is calculated for each latitude from the daily mean rotation rate. Equation (2) in the form

$$[V_{\lambda}] = - \left[\frac{\partial \psi}{\partial \theta} \right]_c \quad (24)$$

determines the corresponding mean value of the meridional streamfunction gradient $[\partial\psi/\partial\theta]_c$. The mean value of $[\partial\psi/\partial\theta]_R$ in relative units of Ψ is obtained from each daily pattern and the normalization factor F computed:

$$F = \frac{[\frac{\partial\psi}{\partial\theta}]_c}{[\frac{\partial\psi}{\partial\theta}]_R} \quad (25)$$

This normalization is then assumed to be constant along the respective latitude and each value of $\partial\psi/\partial\theta$ existing at the individual grid points is adjusted accordingly. The corresponding local zonal velocity components V_λ are computed from Equation (2).

While there is no way to verify that the above method yields realistic magnitudes for the velocity at each point individually, the mean zonal velocity component is that which is observed on a given day. There is no comparable quantity available to determine the magnitude of the meridional component. However, the assumptions upon which the technique is based provide a reasonable approach. Consider again Equation (2) which defines the streamfunction

$$V_\lambda = -\frac{\partial\psi}{\partial\theta} \quad ; \quad V_\theta = \frac{1}{\cos\theta} \frac{\partial\psi}{\partial\lambda} \quad (2)$$

The relationships between the velocity components and their respective streamfunction gradients differ only by the accompanying geometrical factors. At the equator a given streamfunction gradient ought to produce equivalent velocities regardless of orientation.

Considering the appropriate geometrical factors in the present case,

a value for V_{θ} equivalent to V_{λ} at any latitude requires a value of $\partial\psi/\partial\lambda$ which is smaller than the corresponding value of $\partial\psi/\partial\theta$ by a factor of $\cos \theta$. Therefore, Equation (24) relating a given value of $\partial\psi/\partial\theta$ to a known V_{λ} can be modified to apply to the other dimension, i.e.,

$$V_{\theta} = \frac{F}{\cos \theta} \left(\frac{\partial\psi}{\partial\lambda} \right)_R \quad (26)$$

assuming the normalization factor F is constant in two dimensions along the latitude. This procedure assumes that a meridional streamfunction gradient determined from the daily patterns yields a velocity component consistent with a like computation in the zonal direction.

Velocity components in both the meridional and zonal directions were computed as indicated above for a network of gridpoints separated by 4 degrees of latitude and longitude which began at -2 degrees latitude and CMD respectively. Once having calculated the respective velocity components in the above fashion it was a straightforward procedure to determine by linear interpolation, the meridional velocity component corresponding to the position of each sunspot appearing within the confines of the pattern. These meridional velocities appear along with those inferred from sunspot proper motions in Appendix C.

4.2.3. The Statistical Test

Having obtained the necessary estimates of the meridional velocity components to test the validity of the streamfunction patterns, the following

null hypothesis is formulated: The flow patterns obtained by the technique described herein yield meridional velocity components which are completely independent of meridional velocity components for the same location estimated from the daily proper motions of sunspot groups. Since the same quantity is being estimated by two independent methods which should result in a considerable correlation if the technique has any validity at all, the null hypothesis will be accepted or rejected on the basis of a linear correlation analysis.

The linear correlation coefficient for 42 pairs of meridional velocity measurements appearing in Appendix C was calculated according to accepted statistical techniques (c. f., Panofsky and Brier, 1958). A correlation coefficient of 0.34 resulted which was significant at greater than the 1% level of confidence determined by performing an analysis of variance test. Based on this result, the null hypothesis must be rejected and the conclusion reached that some degree of correlation does exist between meridional velocities measured from the flow patterns and sunspot daily proper motions.

It should be pointed out that in performing the above test, one pair of meridional velocities was not included. This pair (spot No. 21 on 01 July) was eliminated due to its close proximity to the sub-earth point -- the point of least reliability when considering the inferred flow patterns. However, the addition of this point to the sample would not have changed the basic conclusion reached. The two data sets were still significantly correlated at greater than the 1% level of confidence although the magnitude of the

correlation was reduced.

Similar judgements concerning the reliability of other pairs of data based on their potential to be influenced by smaller scales of motion could have been made. For example, based on the studies previously cited, the spots exhibiting the fastest motions may have experienced such an effect. Alternatively, the smallest spots appear to have the greatest potential to experience the motions on smaller scales and could be viewed as the most likely candidates for suspicion. An examination of the data presented in Appendix C yields a number of sunspot groups exhibiting these characteristics. However, inspection of the accompanying velocities does not produce uniformly good or bad results. This is not surprising, since even if these particular spots are more under the influence of small scales of motions than motions on the scales the patterns attempt to reproduce, there will be those times during which the two effects will be in phase yielding generally good agreement and those times during which the opposite will be true. It will take a considerably larger data sample than available here to determine the actual conditions. It is interesting to note in passing that several calculations performed after eliminating the least reliable measurements based on the above judgements were attempted and all increased the correlation coefficient to some degree and all continued to be significant at greater than the 1% confidence level.

For example, when the four spots with $\pm 4^{\circ}$ CMD (where components of horizontal motions in the line-of-sight are very small) were eliminated,

the correlation coefficient increased to 0.52. When eliminating from consideration only the six fastest moving spots in the sample (those with latitude differences ≥ 0.5 degrees), the correlation coefficient nearly doubled (0.66). The large increase in the correlation coefficients obtained in each case strongly suggests that inhomogeneities exist in both data sets. However, since the overall data sample is so small, only the one data pair previously identified was not included to avoid unduly weakening the statistics upon which the above test is based.

While the correlation coefficient is a useful tool when judging the overall relationship between two variables, it tends to mask the contribution of each case individually, especially when small amounts of data are involved. As an alternative, the data can be presented in a scatter plot (Figure 10) in which the contribution of each point becomes more obvious. The general trend is apparent with most of the points falling in the two quadrants consistent with a positive correlation. A linear regression line could have been determined for the data but would not have added any additional information.

While the statistical analysis which has been undertaken indicates that there is some degree of information contained in the flow patterns, it remains to determine how these results can be interpreted in terms of the patterns themselves and their representations of the motions in the solar atmosphere. In the present case a highly significant correlation coefficient (0.34) has been obtained -- Is this a good result?

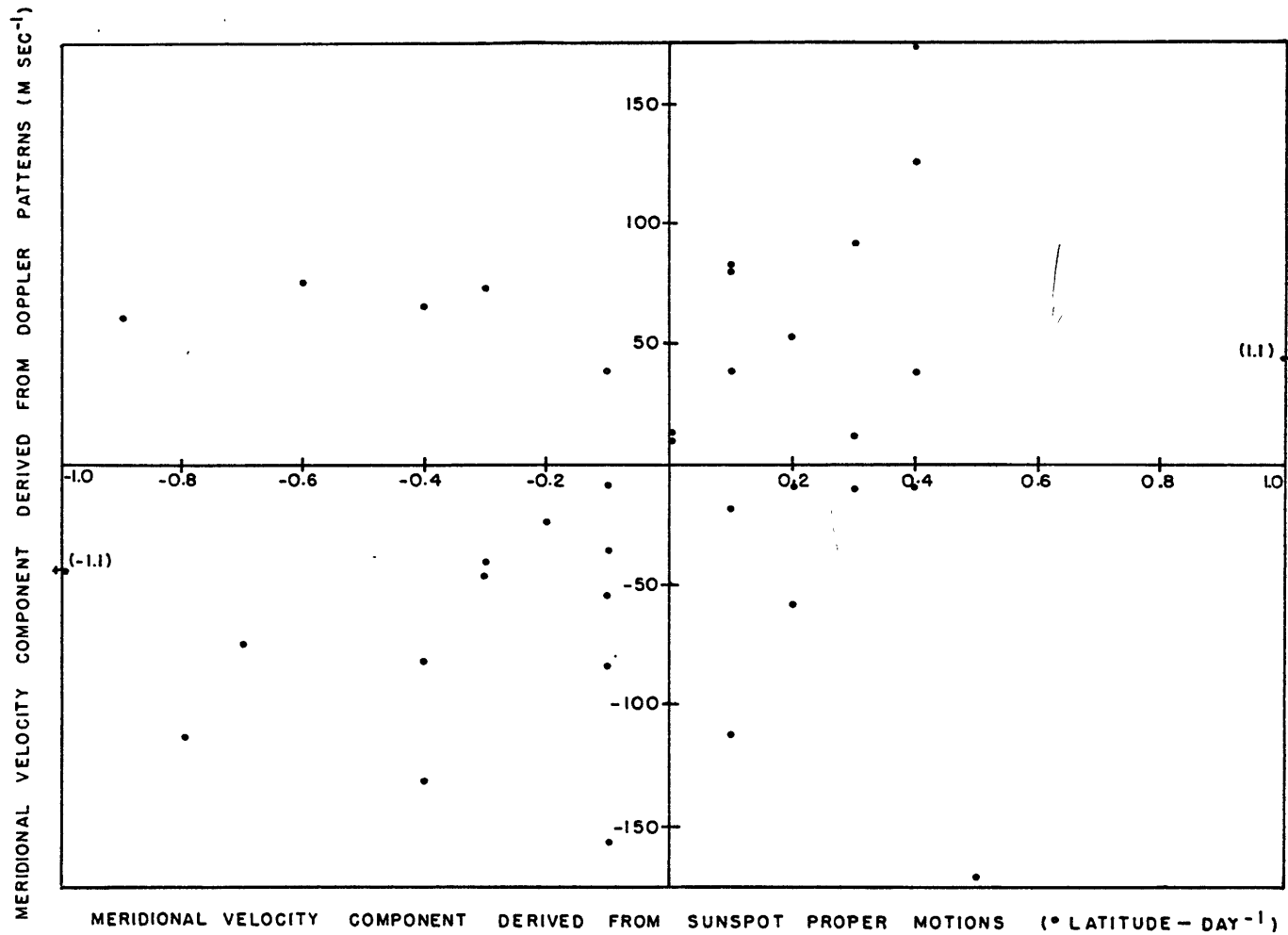


Figure 10. Scatter plot comparing meridional velocity components obtained from the flow patterns with those inferred from the daily proper motion of sunspots.

Clearly, if there was any assurance that the sunspot motions resulted entirely from large-scale motions within the layer represented by the flow patterns, the result would be disappointing. However, as has been previously discussed, there are reasons to believe that any disagreements between the flow patterns and sunspot motions are due in combination to the following four effects.

The first and most obvious are shortcomings in the technique which do not allow a faithful reproduction of the flow in the solar atmosphere. This is one inescapable and perhaps the leading candidate. A second related possibility is the increased suspicion of the flow patterns in the vicinity of active regions due to the presence of organized vertical motions. It is in just these regions where sunspots occur resulting in a comparison with and subsequent judgment based on the least reliable data provided by the patterns. Thirdly, there is evidence to suspect the validity of sunspots as faithful tracers of the flow exhibited by the ambient fluid, e.g., magnetic effects and/or a dynamic interaction may cause relative motion to occur between the spot and fluid bulk. Lastly, recent evidence points to a possibly significant contribution to the daily proper motions of sunspots due to motions on the scale of the convection, this contribution is not uniform but appears to decrease with increasing sunspot size. These latter two possibilities would set an upper limit on the correlation which could exist between the meridional velocities obtained from sunspot motions and those obtained from patterns perfectly representing the large-scale flow.

How do all these possible contributions to the lack of agreement between the two estimates of the meridional velocity components affect the answer to the original question in slightly modified form -- Are these patterns useful when estimating the character of the large-scale flow?

Consider again the results obtained when eliminating the fastest moving spots from the statistical data sample. If these spots contain only a small component of the motion attributed to the large-scale flow, then the correlation coefficient (with respect to the sunspot deduced velocities still imperfectly specified for the other reasons) jumps to 0.66. If the causes of the discrepancies yet remaining are distributed equally between deficiencies in the flow patterns and the shortcomings which still exist when using sunspots as tracers of the large-scale flow, the inferred patterns would represent the actual flow conditions fairly accurately.

The above speculation may be totally unjustified. On the other hand it seems equally unjustified to dismiss as totally useless the flow patterns which have been obtained. These flow patterns, while requiring far more extensive corroboration prior to reaching a final judgment as to their worth, do demonstrate a significant correlation with independent but imperfect estimates of the velocity fields in the solar atmosphere. So it is with guarded optimism that preliminary answers to the questions posed above and in the title of the present chapter are offered -- the first approximation of a technique which infers flow patterns from Doppler

line-of-sight velocity measurements appears to be moderately successful in reproducing motions in the solar atmosphere which are organized on a large scale.

5. Applying the Flow Patterns to Solar Studies

Having tentatively concluded that the flow patterns which have resulted from the technique described herein provide a first approximation to the actual flow in the upper layer of the photosphere, this discussion is now turned to consider a few of the possible contributions which these flow patterns may make to a better understanding of the dynamics of the solar atmosphere. The potential uses are many and it is not the intent of this chapter to present an itemized list. Rather three specific examples are chosen and the results obtained from the data in hand are presented. While necessarily inconclusive, several of the results are extremely interesting and serve to whet the appetite for more of the patterns produced by this newly created analysis tool.

5.1. Formation of Solar Activity Within the Large-Scale Flow

The possibility of a relationship existing between the formation of active regions and the large-scale flow has been considered at various times. For example, Ward in his extensive studies of sunspot motions suspects that the existence of a sunspot itself suggests something "different" about the flow in the vicinity. Starr and Fischer (1971) using mean displacements of leader and follower sunspots suggested that sunspot groups form preferentially in the anticyclonic ridges of the large-scale disturbances. Now that an independent estimate of the large-scale patterns exists, a direct comparison between the location of sunspot groups and features in the large-scale flow field is possible.

Besides the sunspot data used previously in this study, calcium plage measurements provided by McMath-Hulburt Solar Observatory and published in the Solar-Geophysical Data Bulletin will also serve as indications of solar activity. The plage locations while not determined precisely enough to estimate velocities present may serve as a more reliable indicator of the large-scale manifestation of solar activity. As has already been mentioned, the sunspot groups may form preferentially in favorable supergranules which in turn are carried along by the large-scale flow rather than forming in favorable areas with respect to the large-scale flow directly.

The positions of sunspot groups and calcium plages are plotted on the large-scale flow patterns in Figure 11. The number assigned by the respective observatory appears for reference. Each sunspot group is represented by the location of its center of gravity only while the shape and extent of the plage is reproduced as accurately as possible.

The following observations are made upon an examination of Figure 11:

(1) Most smaller scale features in the flow patterns are accompanied by a calcium plage. This is especially true when the feature is located near the center of the disk as on 01-02 July and 08-09 July. A possible link between these smaller scale features and active regions has already been mentioned. However, the suggested association of plages with small-scale features may mark the location of an emerging or

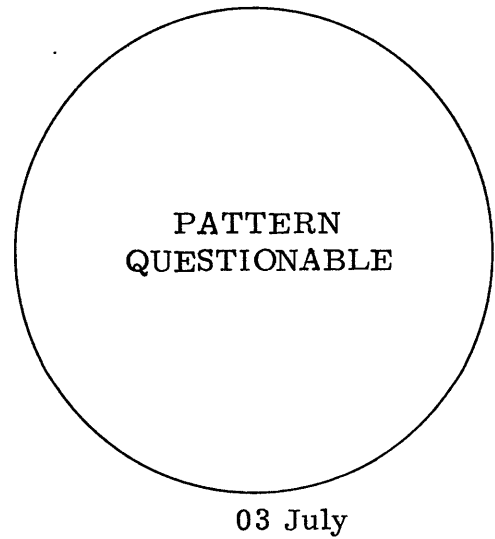
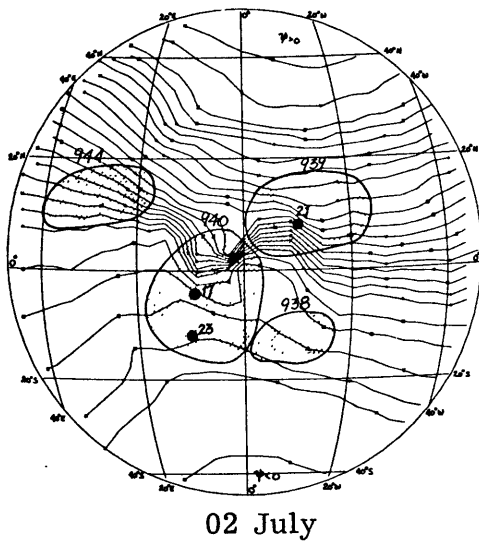
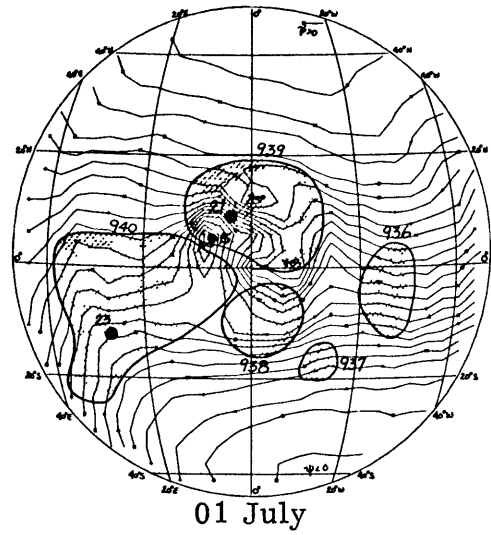
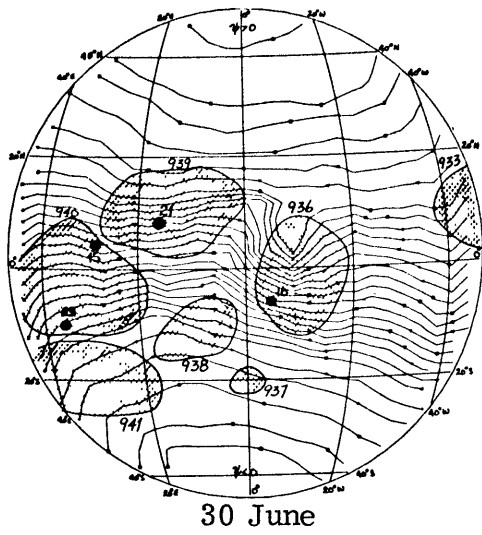
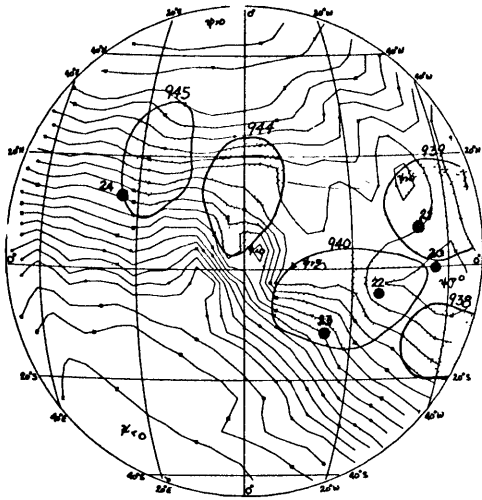
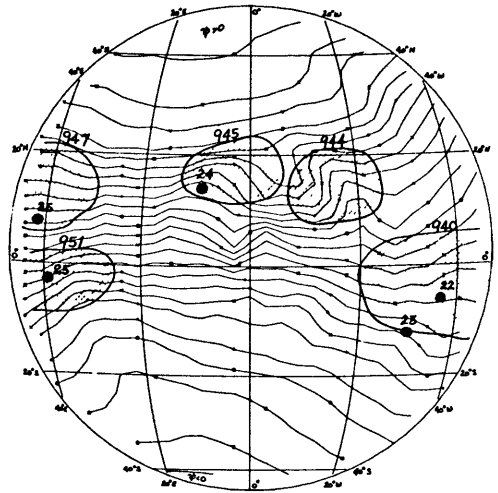


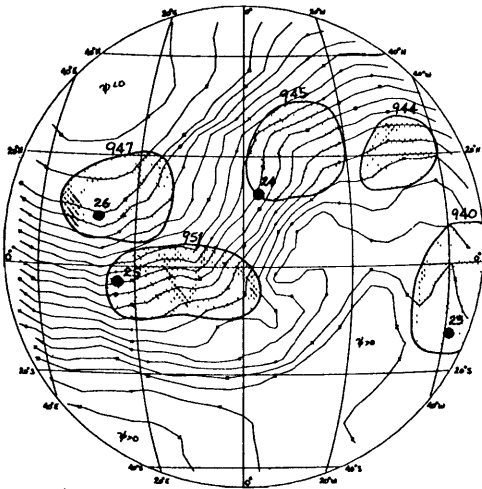
Figure 11. The location of calcium plages and sunspots in the large-scale flow patterns.



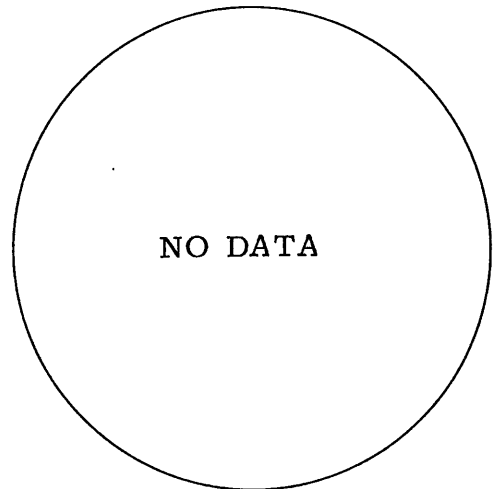
04 July



05 July

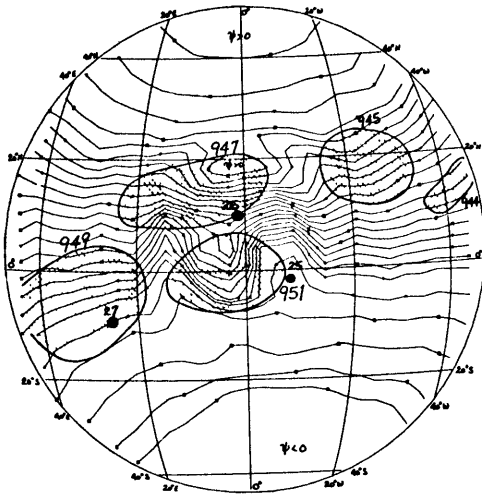


06 July

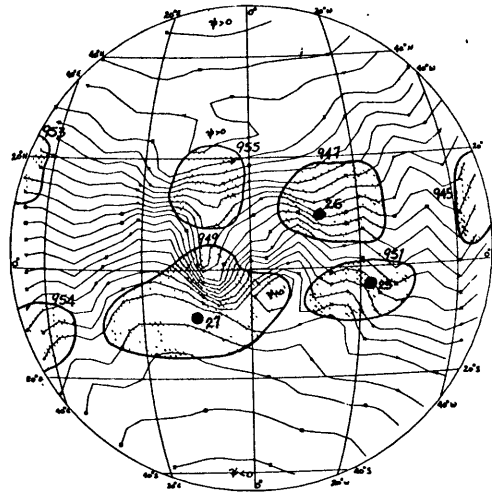


07 July

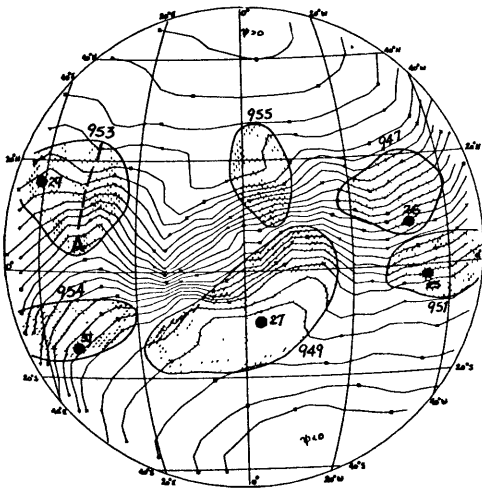
Figure 11. (continued)



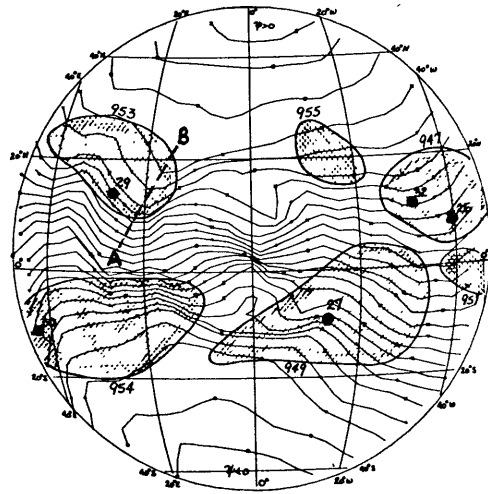
08 July



09 July

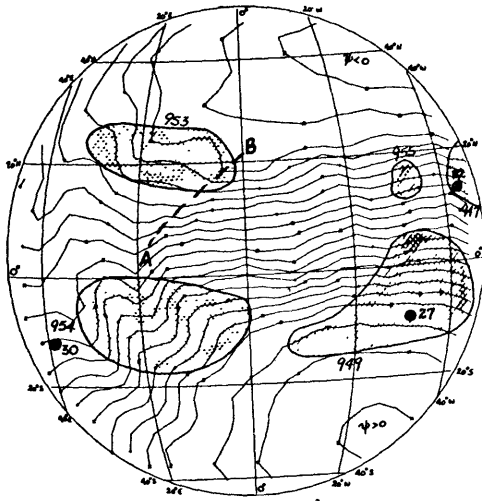


10 July

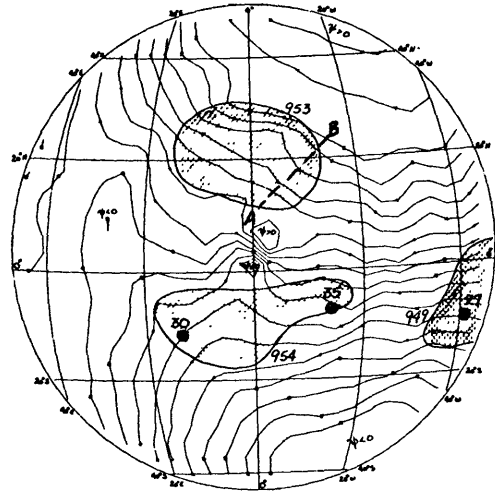


11 July

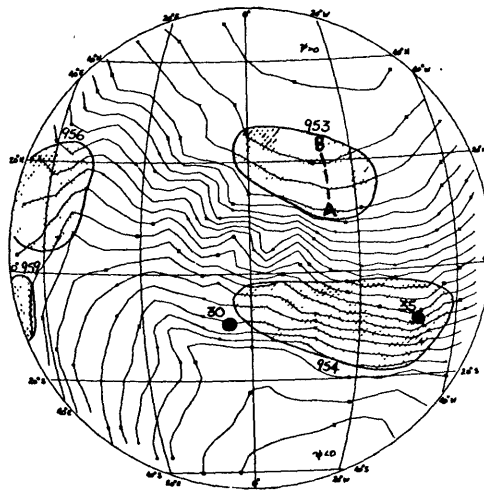
Figure 11. (continued)



12 July



13 July



14 July

Figure 11. (continued)

decaying active region. An example of the latter may exist during the period 10-14 July. Sunspot group number 29 and plage number 953 can be loosely associated with the small wave-like disturbance marked A on 10 July and A, B on later days. On 12 July the sunspot disappears but the plage persists and the wave-like disturbance can still be identified. On the other hand, there are those small-scale features which appear in the flow patterns without a plage nearby.

(2) The sunspots do not appear to be preferentially placed with respect to the large-scale flow pattern. It is sometimes difficult to judge the nature of the large-scale pattern in the vicinity of the active regions and a preference for sunspot formation, if one exists, may first depend on a favorable interaction between the supergranulation and the large-scale flow. It is interesting to note a case on 04 July in particular. During the period 02-04 July a fourth sunspot group formed near one of the three already present on 02 July -- the highly disturbed flow pattern in the western hemisphere on 04 July is striking. A similar sunspot configuration occurs during the period 10-12 July without an accompanying disturbance in the flow field. However, these latter spot groups tend to be smaller than those in the former case and may not have been capable of disturbing the larger scales of motion.

(3) Lastly, and most uncertain is the impression obtained that active regions tend to be most closely associated with the fastest flow and also tend to avoid the semi-permanent circulation centers. Since

active regions and the greatest mean relative velocities are both located between $+30^{\circ}$ latitude generally and the closed centers are poleward of these latitudes, one might argue that such a correspondence would exist if the large-scale flow was somehow randomly produced. This, of course, is true; but the suggested association appears to extend beyond the one based on the long term statistics. A preference for active region (or at least plage) development to occur in the fastest flow seems to hold on a day to day consideration as well.

On one occasion (05-06 July) plages 944, 945, and 947 appeared to be influenced by the shift in the circulation center in the upper left hand quadrant. Both plages 944 and 945 extended poleward more on 06 July than they did on 05 July while plage 947 moved slightly equatorward, all in the general sense of the newly organized flow. Whether this effect is real or the result of the imprecise nature of the plage observations, only time will tell.

The lack of obvious relationships between the observed optical features and the large-scale flow patterns while disappointing is not necessarily unexpected. Studies which have suggested such relationships (e.g., Starr and Fischer) have been based on mean large-scale flow patterns which are consistent with mean sunspot motions and it is not clear how a comparable mean large-scale pattern based on 50 years worth of daily patterns would appear. Alternatively, the unknown but suspected influence of the smaller-scale convection on sunspot formation and

development may preclude any obvious connection with the larger-scales of motion on a day to day basis or, if a link does exist, a more experienced eye may be required to detect it.

5.2. The Dynamics of Active Regions

The study by Starr and Fischer (1971) cited above also concluded that on the average sunspot groups were associated with positive divergence and anticyclonic vorticity as measured by the average relative motions of leader and follower spots themselves. When the sunspot groups are in the early stages of development, the divergence tends to be numerically larger than the vorticity suggesting, as other recent evidence previously cited supports, an influence on spot motions by the underlying convection. As the typical sunspot group ages, the accompanying divergence and vorticity lessen, the former much more so than the latter, to the extent that a general numerical equality is achieved, and at higher latitudes cyclonic vorticity results.

These conclusions were reached using statistics based on a 50 year sample of daily sunspot displacements and as such represent the mean conditions as inferred from motions of spots of all classifications. It would be inappropriate to compare the above quantities with those obtained from the flow patterns with an eye towards making the comparison for any other purpose than simply to estimate the magnitude and sense of the result. Furthermore, any divergent component obtained from the flow patterns cannot represent a real divergence in the flow since the

streamfunction calculations assume nondivergent flow. This leaves only the vorticity as a candidate for further exploration.

Following Starr and Fischer, the divergence and vorticity are, respectively,

$$\frac{\partial u}{\partial x} + \frac{\partial v}{\partial y} \quad \text{and} \quad \frac{\partial v}{\partial x} - \frac{\partial u}{\partial y} \quad (27)$$

where the velocities applicable to the present study are those instantaneous components derived from the flow patterns in the manner described in the previous chapter. The precise velocities used in the finite difference approximation of Equation (27) were those located at the four grid points forming the square 4° on a side which enclosed the sunspot group. This procedure roughly duplicates that of Starr and Fischer who assumed that the leader and follower spots were separated by 4 degrees of longitude and 2 degrees of latitude. The identical sign convention was adopted.

The two quantities (the divergence was calculated as a check) were determined in the vicinity of each spot in the sample of sunspots previously used to validate the flow patterns. Average values of $-0.05 \times 10^{-6} \text{ sec}^{-1}$ and $-1.8 \times 10^{-6} \text{ sec}^{-1}$ were obtained for the divergence and vorticity, respectively. The divergence is nearly two orders of magnitude smaller than the vorticity reflecting the effect of the original nondivergent assumption. That a non-zero value resulted is more than likely attributable to the cartesian coordinate system used when the divergence was being calculated, but as Starr and Fischer justify, "more accuracy is hardly warranted at present".

The magnitude for the vorticity is less than an order of magnitude greater than the value ($\sim 0.5 \times 10^{-6} \text{ sec}^{-1}$) based on 50 years of sunspot motions. Such a difference may be simply traceable to the inaccuracies in the quantitative specification of the pattern-derived velocities, the use of the cartesian coordinate system or some combination of both. Or it could reflect real differences which exist in the vorticity associated with active regions if only more were known concerning the morphology of active regions themselves. Or, it could be due to the scales of motion represented by the two sets of measurements themselves. As has already been discussed, direct use of sunspot displacement data is more apt to reflect motions on scales smaller than those depicted in the flow patterns. Clearly, determining the source of the difference is not possible from the sparse data yielding the present result.

More striking than the numerical difference in the vorticity value determined from the flow patterns was its sense, cyclonic rather than anti-cyclonic. The validity of the sign of the result must also be considered in light of the above considerations. However, fully two-thirds of the individual measurements yielded negative vorticities and of the remainder only two were as large as the absolute value of the mean. It was clear that in this sample at least, negative values were preferred.

Noting this and further stretching the applicability of the flow patterns (hopefully not past their breaking point), a characterization of the flow in the vicinity of active regions can be constructed. Taking stock

of the information available to attempt such a construction reveals that sunspots appear to form at the center of favorable supergranules (Sheeley, 1969) with the attendant upwelling from below and horizontal flow radiating from the spot center. Such a picture is consistent with the positive divergence and anticyclonic vorticity calculated from mean sunspot displacements by Starr and Fischer (1971). These conditions apply to a level in the photosphere near $\tau = 1$.

In the layer between $\tau = 0.004$ and $\tau = 1$ sampled by the Doppler data, downward velocities predominate in the vicinity of active regions (Howard, 1971) while the large-scale flow as just indicated exhibits generally cyclonic vorticity. If a further assumption is made that the smaller scales of motion in this layer are also cyclonic, the flow pattern as depicted in Figure 12 can be constructed. Further speculation as to conditions in the chromosphere will be avoided except to note that material is commonly observed to be falling toward the sunspot along filaments (Zirin, 1966) which are vertical extensions of the enhanced magnetic fields within sunspots.

5.3. Large-Scale Flow Patterns and the Solar General Circulation

Since the deficiencies existing in current models of the solar general circulation were cited in the introduction as partial justification for the current work, this study would not be complete if some consideration was not given to the potential contribution by the large-scale flow patterns to that area. In particular, the series of daily patterns presently available

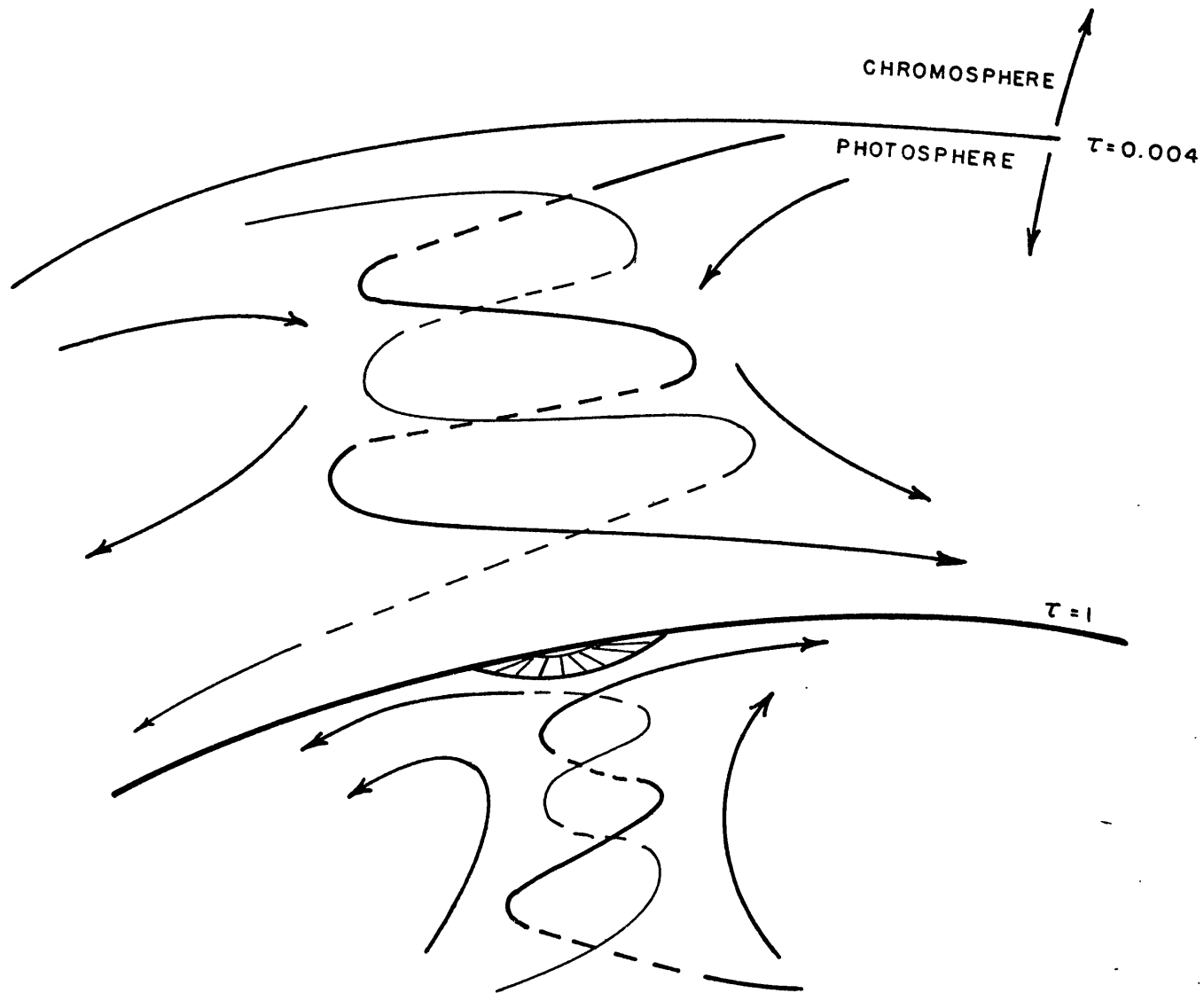


Figure 12. Flow in the vicinity of an active region inferred from various solar measurements.

will be used to estimate the daily transport of momentum by the large-scale motions and its relationship to the observed variations in the daily mean rotation rate. These results will be extended to consider the role of these large-scale motions with respect to other mechanisms which may also contribute to the overall energetics of the solar general circulation.

Until recently the estimates of momentum transport obtained by Ward (1964, 1965a) were interpreted solely in terms of the large scales of motion. This seemed to be appropriate in light of the population of sunspots used to provide estimates of the local velocity fields and the assumptions made concerning the validity of sunspots as tracers of the bulk fluid flow. In light of the recent studies by Starr, Hendl and Ward (1974) and the interpretation of its results by Starr (1974) in terms of the supergranulation effects the appropriateness of Ward's earlier interpretation can be questioned. The slower moving sunspots may still represent the best approximation of the larger scales of motions which sunspots can provide. But the question remains -- "Is this approximation good enough to attribute the entire covariance to the large-scale motions" or, as the current determination of large-scale flow fields suggests, "are even the slower moving sunspots affected appreciably by the smaller scale motions?" If they are, then how does this affect the conclusions previously reached concerning momentum transports as inferred from sunspots and the large-scale flow? An attempt at an answer will be based on a calculation similar to that performed by Ward replacing

daily sunspot displacements with velocities determined directly from the large-scale flow patterns.

The quantity of interest is the covariance of u and v which is directly proportional to the eddy transport of relative angular momentum

$$[u'v'] = [uv] - [u][v] \quad (28)$$

The brackets denote averaging with respect to the segment of the latitude circle represented by the daily pattern. Two major differences exist in the quantity as defined above and the similar quantity used by Ward. The above quantity is determined on a daily basis and only for a segment of the latitude circle while the comparable value considered by Ward represented a long term mean for the complete latitude circle. A determination of an identical long term mean from large-scale flow patterns is possible once a sufficient length of data becomes available.

The exact meaning of the covariance as presently defined is not clear. However, it may be useful as a diagnostic tool to infer the instantaneous transport of angular momentum by the large-scale motions. Furthermore, it will be assumed that the resultant momentum transfer is reflected by an appropriate change in the daily mean zonal velocity which by its nature also applies only to the visible segment of the latitude circle. The validity of these assumptions depends on the degree to which changes in one portion of the solar atmosphere can influence the other. The effects of such interactions are not known. This ignorance extends down to and includes the quantity which is best determined, the mean

rotation rate. From the patterns presented previously it appears as though the determination of the daily mean rotation rate would depend a great deal on the particular longitudinal extent of the atmosphere sampled, a situation equally true for the earth. Studies to determine the instantaneous momentum transport over a portion of a latitude circle similar to the type being considered here are only being begun using terrestrial data. Answers to the questions being raised here may be less uncertain when results of these studies are known.

Nonetheless, the present study will proceed as stated, the potential difficulties acknowledged by assuming that the portion of the atmosphere included within the patterns is representative of the sphere as a whole and exerts an influence on the whole in direct proportion to its fractional part. Under these conditions the covariance defined in Equation (28) can be extended to apply to the complete latitude circle.

The basis for the calculation is the 4° by 4° heliographic grid previously described. The mean zonal and meridional velocity components for each latitude were determined for the longitudinal extent of each daily pattern. Respective covariances for each latitude were then computed. Strictly speaking the covariance determined at a specific latitude reflects the momentum being transported across that latitude circle. However, since such small amounts of data are involved, it seemed to be desirable to improve the estimate of the covariance at the expense of spatial precision. For the sake of comparison the daily momentum transport will be

estimated by covariances determined by two methods. The first estimate will be the covariance obtained for 30° solely (data for both hemispheres are combined). The second will be that value corresponding to the mean of the individual covariances for all grid points between 10° and 30° . The latter value will be interpreted as being proportional to the mean momentum transport across a latitude belt 20° wide.

The daily variations of the covariances and the corresponding mean relative zonal velocity appear in Figures 13 and 14. A point by point comparison strongly suggests that these two quantities are negatively correlated during the period 04 - 13 July. An increase in the magnitude of the covariance is accompanied by a decrease in the mean relative zonal velocity between $+30^{\circ}$ latitude. Especially striking is the general correspondence in magnitude of the two quantities, the two largest covariance values occur on the two days on which the mean relative zonal velocity was less than the long term mean at 20° . This result is more readily apparent when examining the covariances determined for 30° solely than it is for the mean covariance, but it is still true nonetheless. The negative correlation between the covariance and mean relative zonal velocity is more marked when considering the mean covariance for the period 04 - 06 July.

At the beginning of the sample (30 June - 02 July) the two quantities appear to be positively correlated. The sense of the correlation during periods when the effect oscillates from day to day depends to a large degree on the timing assumed for the quantities involved. Recall the

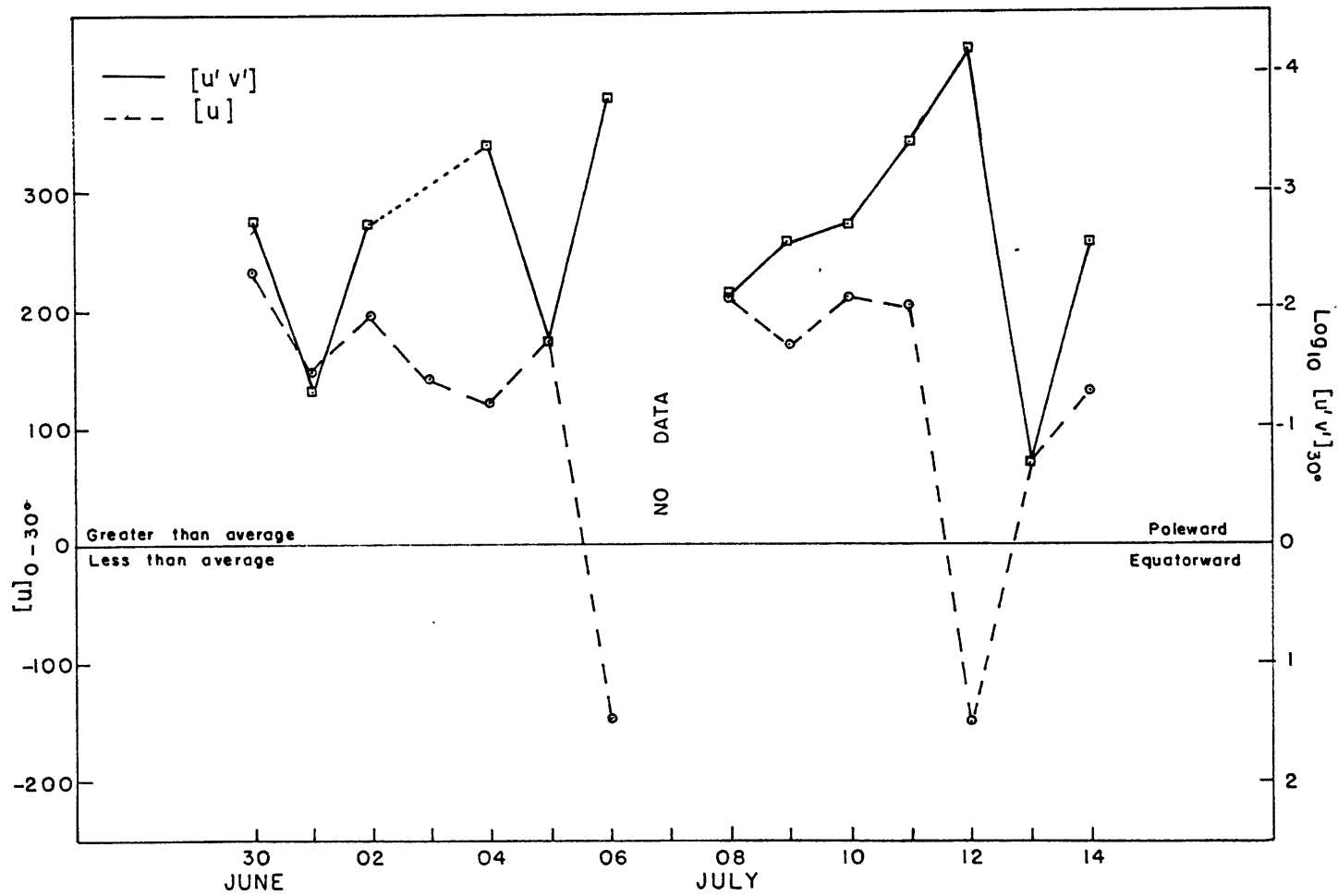


Figure 13. The day to day variation in the mean values of the zonal velocity between $+30^\circ$ latitude and the covariance between the zonal and meridional velocity components at $+30^\circ$ latitude.

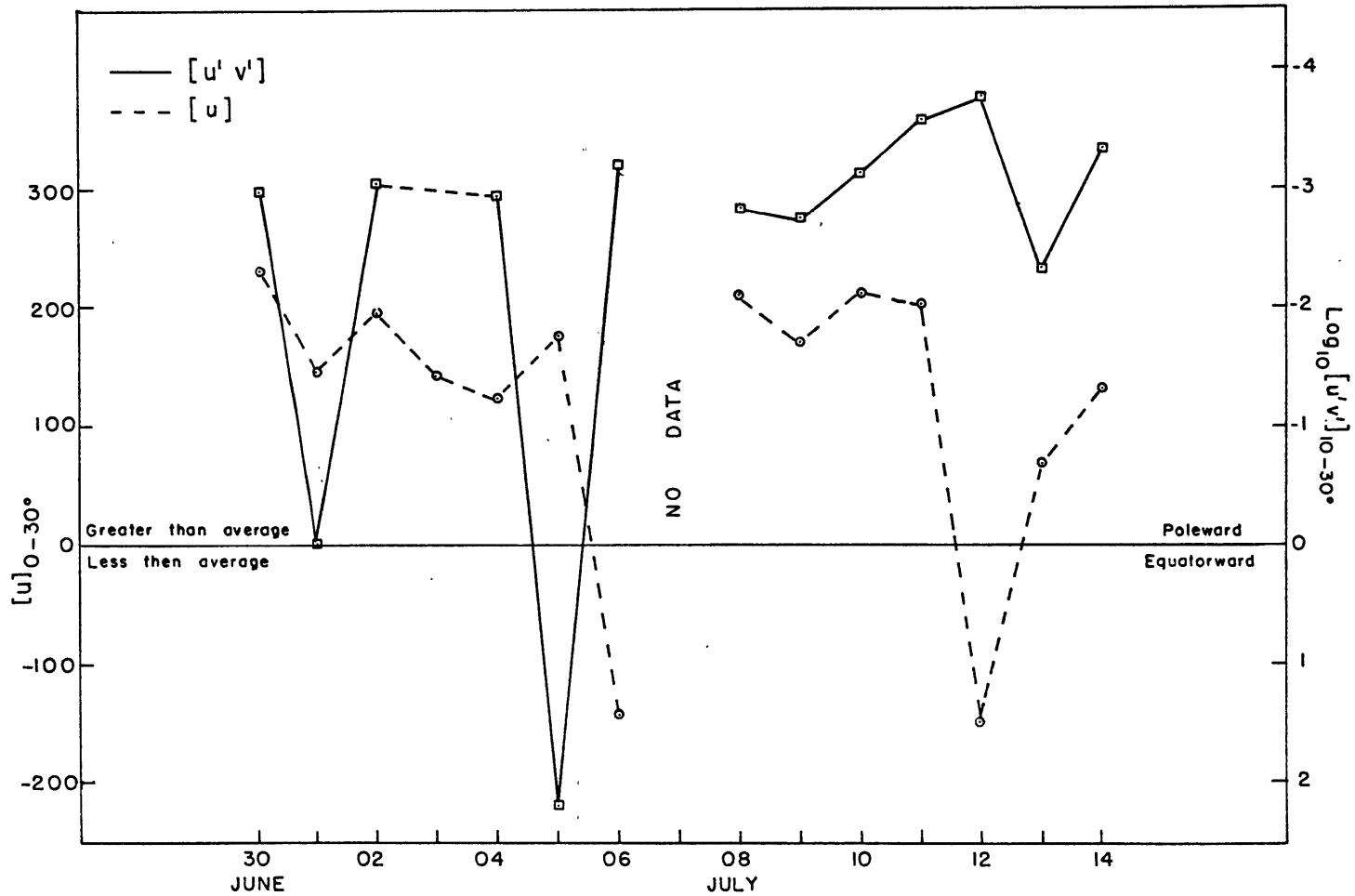


Figure 14. The day to day variation in the mean values of the zonal velocity between -30° latitude and the covariance between the zonal and meridional velocity components which lie within the latitude belt bounded by 10° and 30° in both hemispheres.

manner in which the patterns were produced and verification performed. All the data determined at the time of observation were assumed to be constant until the next observation, an obviously unrealistic but unavoidable procedure. This has already introduced a component of uncertainty when the two independent estimates of the meridional velocity components were compared. The positive correlation during this period may also be due to this imprecise timing.

A more certain interpretation of Figures 13 and 14 must await the collection of much more data than is currently available, but the following sequence of events would be compatible with the preliminary indications. Already mentioned is the equatorward transport of angular momentum which is thought to exist as a result of convection on scales ranging from the size of the postulated and much modelled giant cells down to the size of the observed but until recently discounted supergranulation. Consider the various parts of the entire spectrum of convection as transporting angular momentum in unknown proportions towards the equator building up the equatorial jet. From time to time the jet becomes unstable and the resulting disturbances are organized on a large-scale in such a manner that momentum is transported poleward, reducing the intensity of the jet. Since there is no direct evidence for baroclinicity in the layer being sampled, barotropic instability is the most likely mechanism for producing these large-scale disturbances. Most likely the mean rotation rate determined on a daily basis irregularly oscillates about the long

term mean and represents alternating overcompensation on the part of both simultaneously occurring processes, the convection building the jet to values greater than the long term mean until finally the (barotropic?) instability is able to transport sufficient momentum polewards to reduce the daily mean rotation rate to a value below the long term mean.

To explain the absence of positive covariances it must be remembered that only the large-scale processes are represented by our flow patterns. The large-scale convection would be most accurately represented by the patterns since flows on these scales are most nearly nondivergent. Thus, the covariances calculated from the flow patterns may represent the net transport due to the large-scale convection and the large-scale instabilities. Missing still are the transports (presumably equatorward) contributed by the smaller scales of convection. This missing amount may be sufficiently large to result in positive covariances for days (e.g., 05 and 13 July) on which the mean zonal velocity increases. A completely consistent result comparable to that depicted in Figures 13 and 14 will not be possible until the convection on all scales can be adequately represented. An indirect estimate may be possible by a combination of results similar to these presented here and those obtained by Ward from sunspot motions which most likely also represent the net results of the two competing mechanisms.

The shape of the convective cells and their orientation is a factor which influences the capacity of the cell to transport momentum (Starr,

1974). Presumably some shape and orientation exists which will produce an optimum transport towards the equator. A secondary modulation by the postulated instabilities which develop in the equatorial jet could exist if the instabilities could somehow influence the shape and/or orientation of the convective cells to reduce the direct equatorward transport.

Such a combination of effects could help to explain the rapidity with which these changes occur. These rapid changes raise a question concerning the energy required to effect a typical change. If as Howard and Harvey (1970) suggest, these changes are limited to the layer sampled by the Doppler measurements, then approximately 10^{32} ergs, comparable to the energy released in larger flares, are involved in a typical variation in the mean zonal velocity such as occurred on 11-12 July. Such may be the case. However, if a degree of correspondence does exist between motions in this layer and those obtained from sunspot displacements, the implication is that deeper layers experience a similar variation. If these variations occur over identical intervals in time, satisfying energy requirements within current knowledge may prove to be difficult.

The results of the three pilot studies presented in this chapter were meant to serve as examples of the variety of studies possible using the information provided by the flow patterns. Even if the results are accurate and the conclusions drawn from them wholly valid, they would apply only to the two week period from which the data are drawn. Extending these and other conclusions based on limited data to the conditions

existing in the solar photosphere in general must await similar determinations representing all phases of the solar cycle. There is no reason to believe that the flow patterns obtained during one phase of the solar cycle are typical of those which occur during the other phases. Just the contrary would appear to be the case: the more observations of the solar atmosphere which accrue, the less steady the conditions appear to be.

6. Concluding Remarks

6.1. Summary

A technique has been developed which calculates from Doppler line-of-sight velocity measurements horizontal streamfunctions in the solar photosphere. Whether or not this procedure is capable of performing the intended task and of subsequently producing a valid approximation of the flow patterns has been judged from both a qualitative and a quantitative standpoint.

Qualitatively, the appearance and continuity displayed by a two week sample of results suggests that the technique has some degree of credibility. An inspection of the results for this period yields the following observations concerning the flow patterns:

(1) Flow in the solar photosphere appears to be organized on a large scale and exhibits certain characteristics of a large-scale eddy regime, i. e., the presence of circulation centers accompanied by a meandering high velocity stream.

(2) The circulation centers reflect the sense of the solar rotation although the rate is somewhat less than the underlying reference rate. This difference may be caused by a positional bias towards the center of the disk due to geometrical foreshortening, the data averaging technique and/or an actual retardation, for example, if Rossby-wave dynamics were applicable.

(3) Smaller scale perturbations become more pronounced when an

active region is in the vicinity of the sub-earth point. Such disturbances in the large-scale flow may represent real small-scale motions for the most part, but it is probable that an additional spurious component is present due to net downward motions which have been observed to occur in conjunction with active regions. These downward motions are most readily observed near the center of the disk where the line-of-sight component of the horizontal motion is smallest. Additionally, since the area over which the data are averaged is smallest near the sub-earth point, a non-zero contribution to the mean line-of-sight velocity from a net vertical motion is most likely to occur in this region. Both effects would contribute to a spurious component in the horizontal streamfunction. Hence, within the patterns themselves the least reliability occurs in the vicinity of active regions when they occur near the sub-earth point.

(4) On occasion, rather significant changes occur in the day to day appearance of the patterns themselves. On two occasions, the mean rotation rate at all latitudes was less than the underlying reference rotation rate yielding mean easterlies on those days.

A quantitative estimate of the technique's validity was based on a comparison between the meridional velocity components obtained from the patterns themselves and those estimated from the daily proper motions of sunspots. A linear correlation coefficient of 0.34 was found to exist between these two independently obtained velocity components.

Evidence is cited which suggests that sunspots are not entirely

accurate tracers of the flow in which they are embedded. Magnetic effects, dynamic interaction between the spot and the ambient fluid and other possibilities cause sunspots to respond to motions in the surrounding fluid in a variable, imperfect and largely unknown manner. Furthermore, results of a recent study indicate that sunspots, especially smaller ones, may be responding more to the higher velocities organized on smaller scales associated with convection. When the meridional velocity pairs associated with the six fastest moving spots were set aside, the correlation coefficient nearly doubled ($= 0.66$). Thus, it is possible that even a perfect representation of the large-scale flow would yield velocities which would not correlate perfectly with those estimated from sunspot motions. With this in mind the uncorrelated component was assumed to be due to the uncertainties which exist within the flow patterns themselves and those introduced when using sunspot motions to estimate local velocity fields. The effect on the final result due to each uncertain source is not known. After considering the strengths and weaknesses in the foregoing analyses, it was concluded that the flow patterns produced are better than the correlation coefficient obtained might indicate and represent a useful first approximation to the actual flow fields in the solar photosphere.

Several possible sources of error exist which affect the reliability of the original measurements. The velocities which the measurements provide are relative ones reckoned with respect to a daily determined

reference level. Strong motions in either direction concentrated in relatively small areas can change the reference level which then affects motions at other locations. Significant changes in the atmospheric pressure during the course of an observation can produce a systematic drift in the reference level. An increase in the averaged line-of-sight velocities limbwards of 0.8 central distance exists in the data analyzed in this study. The cause of this effect is unknown but may be linked to an inadequate red shift correction. Due to this increase the analysis was terminated at 0.8 central distance.

Results of three pilot studies demonstrate the various applications of these patterns to the overall investigation of solar phenomena. The following conclusions are of necessity very tentative due to the dearth of data upon which they are based. The first study compared the locations of calcium plages and sunspots with features in the large-scale flow patterns. While no definitive relationships could be found, there was a tendency for plages to be located in conjunction with small-scale features in the large-scale flow. Their day to day motions appeared to be influenced by changes in the large-scale flow. Even more uncertain was the conclusion reached that the plages tended to be located within the fastest portions of the instantaneous flow. The tenuous nature of plages themselves introduces a further uncertainty into the present conclusions.

No similar associations could be found between the sunspots and the large-scale flow which may be the result of a smaller scale influence.

One interesting situation did occur with respect to sunspots, however, the presence of four spots within a restricted area coincided with the occurrence of small-scale disturbances over an unusually extensive region. Whether or not this disturbed flow resulted from the combined effect of the four spots is impossible to judge at this time.

The remaining two studies used the flow patterns to estimate the vorticity in the vicinity of sunspots and the momentum transported by the large-scale features. Recall that sunspots reflect the motions in a layer beneath that sampled by the Doppler measurements. The vorticity calculated from the flow patterns and that determined from the mean motions of individual spot pairs were of the same magnitude. However, the sense of rotation was opposite, that determined from sunspot motions was anticyclonic, while the patterns yielded cyclonic flow. Based on other facts concerning sunspot formation, i. e., the relative depths involved and the mean vertical motions thought to exist at the two levels, a consistent picture of the flow in the vicinity of an active region was synthesized. Such a flow involves an anticyclonic upward motion at levels below the sunspot accompanied by downward cyclonic flow in the layer sampled by the Doppler measurements with a divergent, nearly horizontal flow at an intermediate level.

Momentum transports were approximated by calculating the covariances existing between the meridional and zonal velocity components obtained from the patterns. Two estimates of the covariance were

obtained; one for $+30^{\circ}$ latitude solely and the other for a belt between 10° and 30° latitude (both hemispheres combined). In almost all cases the resulting covariance was negative, implying a poleward transport of momentum by the scales of motions inferred from the flow patterns. A comparison between day-to-day changes of the covariances (and hence the momentum transports) and the mean zonal velocity between $+30^{\circ}$ latitude strongly suggested that a negative correlation exists between the two, i.e., on successive days when the covariance between the meridional and zonal velocity components increased (implying an increase in the momentum transported across $+30^{\circ}$ latitude polewards), the mean zonal velocity decreased and vice versa. The two days on which the mean zonal velocity was less than the reference rotation rate were accompanied by the two greatest negative covariances.

This result was considered in addition to the other mechanisms, e.g., convection on scales down to the supergranulation which are thought to transport momentum equatorwards. The following possibility exists. Convection associated with various vertical instabilities produces a horizontal flow pattern which transports momentum equatorwards, building up the equatorial jet. When the magnitude of the jet reaches some critical point, an instability occurs which perturbs the previous pattern and creates a large-scale disturbance which transports momentum polewards and reduces the mean zonal velocity near the equator. The nature of the instability is unknown but since there is no evidence to suggest

baroclinicity within the layer, barotropic instability is a possibility. The barotropic instability then acts as a modulator keeping the mean zonal velocity between two extreme values. Since the horizontal orientation of the convection units may affect the magnitude of the equatorward transport of momentum, the large-scale flow could also directly affect the equatorward momentum transport by changing the mean orientation of the convective cells. The combined result may help to explain the rapid changes which are observed.

6.2. Suggestions for Future Work

The technique which has been developed by the present effort represents only a first attempt at specifying the large-scale velocity fields. It is suggested that any future work be conducted at Mt. Wilson Observatory to enable not only a more timely production of the daily flow patterns but to allow future versions of the technique to benefit from possible improvements resulting from an intimate knowledge of the instrumentation and data reduction methods employed. Such familiarity is possible only if daily contact with the overall data acquisition process is maintained. Future work ought to proceed along three fronts simultaneously.

The most obvious extension of the present work is to apply the technique as it stands to a much larger volume of data. The tentative nature of all the results presented here makes such an extension a minimum requirement if for no other purpose than to verify the current judgment on the capability of the technique. Beyond this necessary but

somewhat unprogressive goal is the extension of the studies in a way so as to uncover unknown facts and correct current misconceptions. The amount of data necessary to reach new conclusions will undoubtedly vary and may encompass several solar cycles when studying the more complex processes. Thus it would be most advantageous to begin as soon as possible to acquire data on a regular basis.

Beyond the requirement to simply extend the current analysis is the necessity for continual improvement in the analysis technique itself. The continued production will provide clues as to how best to accomplish these improvements, but immediate possibilities include upgrading the analysis, for example in the vicinity of the sub-earth point especially when active regions are present. This may require the introduction of a velocity potential if an adjustment in the area over which data averaging occurs does not adequately remove the effects of organized vertical motions. Some consideration should be given to including persistence in the subsequent pattern if it appears that persistence plays a significant role over a long enough period of time. Furthermore, extending the analysis to include the entire disk should be attempted. Such an improvement may have to await the identification and removal of the factor causing the annulus average to increase limbwards of 0.8 central distance, if such an inhomogeneity remains in the data.

Perhaps the greatest potential for an improved product are more precise observations. Several sources of uncertainty in the data have

been discussed which probably have a considerable effect on the daily patterns. The addition of an absolute wavelength standard to the instrument which will allow absolute velocities to be measured will represent a marked improvement in the quality of the observations. No longer would the Doppler line-of-sight velocities be dependent on uncertain reference levels, instrumental corrections and changes in the atmospheric pressure. Other improvements to the observational procedure and data reduction techniques may well be suggested by the future improvements in the patterns themselves to the mutual benefit of both.

These suggestions represent but a few of the improvements which will undoubtedly be necessary to perfect the technique. Although it is recognized that the patterns in their present form represent the crudest first approximation of the local velocity fields in the solar photosphere, it is hoped that they may serve to stimulate sufficient interest in their potential to encourage their continued evolution and subsequent application to the many unsolved problems in the field of solar physics.

Appendix A

Velocity Components Relative to Integration Paths

The flow pattern which results from the analysis is independent of the manner in which the streamfunctions were determined. Therefore, the pattern produced can be used to calculate velocities with respect to any appropriately defined coordinate system. For the purposes of relating the arbitrary constants of integration, velocity components relative to a spherical coordinate system are used with the coordinates defined such that one axis corresponds to a line connecting the sub-earth with the center of the sun. For two-dimensional, nondivergent flow in this system

$$\vec{\nabla} \cdot \vec{V} = \frac{1}{r^2 \sin \varphi} \left[\frac{\partial (V_\varphi r \sin \varphi)}{\partial \varphi} + \frac{\partial (V_\alpha r)}{\partial \alpha} \right] = 0 \quad (A1)$$

where V_φ and V_α are the velocity components normal and tangential to the integration path. A streamfunction is then defined such that

$$\frac{\partial \Psi}{\partial \alpha} = V_\varphi r \sin \varphi \quad , \quad \frac{\partial \Psi}{\partial \varphi} = -V_\alpha r \quad (A2)$$

or since $r = \sin \varphi$ (with $R = 1$),

$$\frac{\partial \Psi}{\partial \alpha} = V_\varphi \sin^2 \varphi \quad (a) \quad , \quad \frac{\partial \Psi}{\partial \varphi} = -V_\alpha \sin \varphi \quad (b) \quad (A3)$$

The line-of-sight component of V_φ is the entire velocity as measured from the earth since V_α is wholly normal to the line-of-sight.

Therefore, (A3 - a) is actually the differential form of Equation (5) in

the text since $V_\ell = V_\varphi \sin \varphi$ and $ds = \sin \varphi d\alpha$. From (A3 - b) it

follows directly that $V_\alpha^* = 0$ when $\frac{\partial \Psi^*}{\partial \varphi} = 0$.

Appendix B

Calculation of Average Velocity in Annulus Due to

Position of Sub-Earth Point

Consider the paths of integration to be the intersection of a sphere and plane. The equation of the plane in X , Y , Z coordinates is

$$Z = -\cot B_0 (Y - \cos \varphi \sec B_0) \quad (B1)$$

where B_0 and φ are the latitude of the sub-earth point and central angle respectively and $R=1$. When viewed along the Y -axis these circles become ellipses and the latitudes straight lines. Since the tangential velocity around the circles due to the mean differential rotation relative to $+20^\circ$ latitude is not foreshortened when $B_0 \neq 0$, the tangential velocity around the elliptical projections is equivalent. It remains to calculate the angle between the intersection of the ellipse and latitude circles.

In the $X-Z$ plane, the ellipses are described by

$$X^2 + (Z - \cos \varphi \sin B_0)^2 = \cos^2 B_0 \sin^2 \varphi \quad (B2)$$

and the latitudes by $Z = \text{constant}$. The tangent of the angle formed at the intersection of these curves is

$$\frac{dZ}{dX} = \tan \gamma = - \frac{X}{Z - \cos \varphi \sin B_0} \quad (B3)$$

A net counterclockwise flow around the ellipse is defined to be positive requiring the angle formed by the intersection of the two curves to be 0° at the southern point of tangency and increase in the counterclockwise sense. Thus, when $B_0 > 0$, the net flow will be positive and vice versa.

Appendix B (continued)

Once the angle between the two curves is determined the tangential component due to the differential rotation (relative to $+20^\circ$ latitude) can be calculated. The velocity along the solar surface corresponding to this differential rotation is

$$V_{DR} = (\omega_{\Theta} - \omega_{20^\circ}) R \cos \Theta \quad \text{m-sec}^{-1} \quad (\text{B4})$$

where ω_{Θ} and ω_{20° are the mean rotation rates (in sec^{-1}) at Θ and 20° latitude, respectively. R is the radius of the sun, $6.96 (10^8)$ meters.

The tangential component of V_{DR} around the paths of integration is

$$V_{\alpha} = V_{DR} \cos \gamma \quad \text{m-sec}^{-1} \quad (\text{B5})$$

This component was determined for each degree of latitude which intersected a given ellipse and a mean V_{α} , V_{α}^* , calculated.

Utilizing a relationship developed in Appendix A, i. e., (A3-b), the change in the mean streamfunction on a given path, $\Delta\psi^*$, can be computed since

$$\Delta\psi^* = -V_{\alpha}^* \sin \varphi_m \Delta \varphi \quad (\text{B6})$$

where φ_m is the central angle of the annulus midpoint. Here a positive $\Delta\psi^*/\Delta\varphi$ corresponds to a negative (clockwise) net flow and vice versa.

Appendix C

Sunspot and Meridional Velocity Data

<u>Date</u>	<u>RGO No.</u>	<u>Latitude</u>	<u>CMD</u>	<u>Meridional Velocities</u>	
				<u>Sunspot</u>	<u>Flow Pattern</u>
30 June	21	7.8	-17.8	30	48
	15	5.0	-26.4	110	44
	23	-13.6	-36.9	-30	75
01 July	21	7.5	-4.5	-10	137
	23	-13.9	-23.8	30	11
02 July	21	7.6	9.8	10	156
	23	-13.6	-10.9	0	28
04 July	20	0	38.5	-20	-10
	21	7.1	36.5	40	86
	22	-5.2	24.5	-70	-73
	23	-13.6	14.6	-10	-93
	24	13.6	-21.3	10	84
05 July	22	-5.9	38.8	10	42
	23	-13.7	28.1	10	-14
	24	13.5	-9.8	-40	-130
	25	-3.5	-39.2	10	82
	26	8.4	-41.0	-30	11
06 July	23	-13.6	41.0	0	25
	24	13.9	3.2	-50	190
	25	-3.4	-22.9	-30	-34
	26	8.7	-27.4	80	-10
08 July	25	-3.6	7.2	30	47
	26	8.9	-0.8	60	-20
	27	-9.9	-24.6	40	64

Appendix C (continued)

<u>Date</u>	<u>RGO No.</u>	<u>Latitude</u>	<u>CMD</u>	<u>Meridional Velocities</u>	
				<u>Sunspot</u>	<u>Flow Pattern</u>
09 July	25	-3.3	21.6	10	-114
	26	8.3	13.3	0	-30
	27	-9.5	-11.3	-40	-127
10 July	25	-3.2	34.5	110	39
	26	8.3	26.5	-10	-84
	27	-9.9	2.6	40	117
	29	15.8	-40.5	-20	-52
11 July	25	-2.1	44.6	-30	80
	26	8.4	39.9	40	-64
	27	-9.5	15.9	0	-52
	30	-11.5	-42.7	0	192
12 July	27	-9.5	29.2	40	-8
	30	-11.5	-39.4	20	-5
	32	12.3	42.9	90	-61
13 July	27	-9.1	41.8	-20	-10
	30	-11.3	-16.5	-10	55
	35	-8.6	14.6	-10	-31
14 July	30	-11.4	-3.1	-10	-7
	35	-8.7	28.1	-20	-23

NOTE: Positive (negative) velocities denote equatorward (poleward) motion in both hemispheres.

ACKNOWLEDGMENTS

I am indebted to Professor Victor P. Starr for providing guidance, inspiration and numerous bits of insight during the completion of this study.

My thanks go to Dr. Robert Howard of Mt. Wilson Observatory for providing the Doppler velocity data upon which this study is based and to Mr. P.S. Laurie of the Royal Greenwich Observatory for providing the sunspot measurements. Also, I would like to thank Miss Patricia Bench of the Air Force Cambridge Research Laboratories for her programming assistance, Mrs. Barbara Goodwin for typing the manuscript and my colleagues, especially Dr. R.D. Rosen, for their many helpful discussions.

To Dr. Fred Ward of AFCRL go my special thanks, not only for his technical assistance, but for his friendship, constant encouragement and advice.

Finally, I am most grateful of all to my wife and family for their unyielding support and understanding especially during the many times I tried their patience.

My financial support while at M.I.T. was provided by the Air Force Cambridge Research Laboratories, Air Force Systems Command, Contract No. F19628-72-C-0002.

REFERENCES

- Adam, M.G., 1959: A new determination of the center to limb change in solar wave-lengths. Mon. Not. Roy. Astron. Soc., 119, 460-474.
- Allen, C.W., 1963: Astrophysical Quantities. The Athlone Press, London, 291 pp.
- Aller, L.H., 1963: Astrophysics: The Atmospheres of the Sun and Stars. The Ronald Press Co., New York, 650 pp.
- Altrock, R.C. and R.C. Canfield, 1972: Observations of photospheric pole-equator temperature differences. Solar Phys., 23, 257-264.
- Busse, F.H., 1970: Differential rotation in stellar convection zones. Astrophys. J., 159, 629-639.
- Canfield, R.C., 1973: Observations of the variation of temperature with latitude in the upper solar photosphere II. Magnetic field comparison, implications for solar oblateness measurements and harmonic analysis. Astrophys. J., 179, 643-650.
- Cocke, W.J., 1967: On the solar differential rotation and meridional currents. Astrophys. J., 150, 1041-1050.
- Davies-Jones, R.P. and P.A. Gilman, 1970: On large-scale solar convection. Solar Phys., 12, 3-22.
- Durney, B., 1972: On the sun's differential rotation and pole-equator temperature difference. Solar Phys., 26, 3-7.

- Durney, B., 1974: On the sun's differential rotation: its maintenance by large scale meridional motions in the convective zone. Astroph. J., 190, 211-222.
- Durney, B.R. and I.W. Roxburgh, 1971: Inhomogeneous convection and the equatorial acceleration of the sun. Solar Phys., 16, 3-20.
- Fischer, H.J.E., 1971: Test of a solar streamline analysis on terrestrial wind data. Solar Phys., 20, 26-30.
- Gilman, P.A., 1969: A Rossby-wave dynamo for the sun. I. Solar Phys., 8, 316-330, II. Solar Phys., 9, 3-18.
- _____, 1971: A method for constructing streamlines for the sun's large scale flow from Doppler velocities. Solar Phys., 19, 40-43.
- _____, 1972: Nonlinear Boussinesq convective model for large scale solar circulations. Solar Phys., 27, 3-26.
- _____, 1974: Solar rotation. Annual Review of Astronomy and Astrophysics, 12, in press.
- Gordon, C.T., 1972: Design of a numerical solar dynamo model. Final Report, AF Contract F19628-69-C0042, Dept. of Meteorology, MIT.
- Hart, A.B., 1954: Motions in the sun at the photospheric level IV. The equatorial rotation and possible velocity fields in the photosphere. Mon. Not. Roy. Astron. Soc., 114, 17-38.
- _____, 1956: Motions in the sun at the photospheric level VI. Large scale motions in the equatorial region. Mon. Not. Roy. Astron. Soc., 116, 38-55.

- Hart, M.A., 1974: An explanation of the solar limb shift. Astrophys. J., 187, 393-401.
- Heard, W.B. and Veronis, G., 1974: J. Fluid Mech., in press.
- Howard, R., 1971: The large-scale velocity fields of the solar atmosphere. Solar Phys., 16, 21-36.
- _____, 1972: The velocity fields in active regions. Solar Phys., 24, 123-128.
- _____, 1973: Study to extend the knowledge of solar active regions and associated phenomena. Air Force Cambridge Research Laboratories, Report TR-73-0120.
- Howard, R. and J. Harvey, 1970: Spectroscopic determinations of solar rotation. Solar Phys., 12, 23-51.
- Howard, R., A.S. Tanenbaum and J.M. Wilcox, 1968: A new method of magnetograph observation of the photospheric brightness, velocity and magnetic fields. Solar Phys., 4, 286-299.
- Kato, S., 1969: The excitation of nonspherical waves in differentially rotating stellar convective envelopes. Astrophys. J., 157, 827-834.
- Kato, S. and Y. Nakagawa, 1969: The solar differential rotation and Rossby-type waves. Solar Phys., 10, 476-493.
- _____, 1970: Excitation of non-spherical waves in solar atmosphere in the presence of toroidal magnetic field. Solar Phys., 14, 138-146.

Kinman, T. D. , 1953: Motions in the sun at the photospheric level III.

The Evershed effect in sunspots of different sizes. Mon. Not. Roy. Astron. Soc., 113, 613-634.

Kippenhahn, R., 1963: Differential rotation in stars with convective envelopes. Astrophys. J., 137, 664-678.

Livingston, W.C., 1969: Solar rotation, 1966-68. Solar Phys., 7, 144-146.

Nakagawa, Y. and Priest, E.R., 1973: The energy spectrum of small-scale solar magnetic fields. Astroph. J., 179, 949-963.

Newton, H.W. and M.L. Nunn, 1951: The sun's rotation derived from sunspots 1934-1944 and additional results. Mon. Not. Roy. Astron. Soc., 111, 413-421.

Panofsky, H.A. and G.W. Brier, 1958: Some Applications of Statistics To Meteorology. Mineral Industries Extension Service, University Park, Pa., 224 pp.

Piddington, J.H., 1971: Large-scale motions in the sun. Solar Phys., 21, 4-20.

Plasket, H.H., 1952: Motions in the sun at the photospheric level I. Methods. Mon. Not. Roy. Astron. Soc., 112, 414-424.

_____, 1954: Motions in the sun at the photospheric level V. Velocities of granules and of other localized regions. Mon. Not. Roy. Astron. Soc., 114, 251-270.

Plaskett, H.H., 1959: Motions in the sun at the photospheric level VIII.

Solar rotation and photospheric circulation. Mon. Not. Roy. Astron. Soc., 119, 197-212.

_____, 1966: The polar rotation of the sun. Mon. Not. Roy. Astron. Soc., 131, 407-433.

Sheeley, N.R., 1969: The evolution of the photospheric network, Solar Phys., 9, 347-357.

Simon, G.W. and R.B. Leighton, 1964: Velocity fields in the solar atmosphere III. Large-scale motions, the chromospheric network and magnetic fields, Astrophys. J., 140, 1120-1147.

Starr, V.P., 1968: Physics of Negative Viscosity Phenomena. McGraw-Hill Book Co., New York, 256 pp.

_____, 1973a: The parameterization of dynamic processes. Tellus, 25, 219-223.

_____, 1973b: A preliminary dynamic view of the circulation of Jupiter's atmosphere. Pure and Appl. Geophys., 110, 2108-2129.

_____, 1974: Does the solar supergranulation transport angular momentum equatorward? Submitted to Tellus.

Starr, V.P. and H.J.E. Fischer, 1971: Active regions and the large scale flow in the solar photosphere. Pure and Appl. Geophys., 92, 219-232.

Starr, V.P. and P.A. Gilman, 1965a: Energetics of the solar rotation. Astrophys. J., 141, 1119-1125.

- Starr, V.P. and P. A. Gilman, 1965b: On the structure and energetics of large scale hydromagnetic disturbances in the solar photosphere. Tellus, 17, 334-340.
- Starr, V.P., R.G. Hendl and F.Ward, 1974: To be published.
- Stenflo, J. O., 1972: Evolution of solar magnetic fields over an 11-year period. Solar Phys., 23, 307-339.
- Suess, S.T., 1971: Planetary waves on the sun? Solar Phys., 18, 172-175.
- Ward, F., 1964: General circulation of the solar atmosphere from observational evidence. Pure and Appl. Geophys., 58, 157-186.
- _____, 1965a: The general circulation of the solar atmosphere and the maintenance of the equatorial acceleration. Astrophys. J., 141, 534-547.
- _____, 1965b: The effect of some systematic errors in the determination of the general circulation of the solar atmosphere. Pure and Appl. Geophys., 60, 126-128.
- _____, 1966a: Determination of the solar rotation from the motion of identifiable features. Astrophys. J., 145, 416-425.
- _____, 1966b: The longitudinal proper motion of sunspots and the solar rotation rate. Pure and Appl. Geophys., 63, 196-204.
- _____, 1967: Comments on Plaskett's "The polar rotation of the sun". Mon. Not. Roy. Astron. Soc., 135, 147-148.

- Ward, F., 1973: The latitudinal motion of sunspots and solar meridional circulations. Solar Phys., 30, 527-538.
- Wilcox, J.M. and D.S. Colburn, 1969: Interplanetary sector structure in the rising portion on the sunspot cycle. J. Geophys. Res., 74, 2388-2392.
- Wilcox, J.M. and R. Howard, 1968: A large-scale pattern in the solar magnetic field. Solar Phys., 5, 564-574.
- _____, 1970: Differential rotation of the photospheric magnetic field. Solar Phys., 13, 251-260.
- Yoshimura, H., 1971: Complexes of activity of the solar cycle and very large scale convection. Solar Phys., 18, 417-433.
- Zirin, H. 1966: The Solar Atmosphere. Blaisdell Publ. Co., Waltham, Mass., 502 pp.

BIOGRAPHICAL NOTE

The author was born on 23 March 1941 in Hoboken, New Jersey and received his primary and secondary education in North Bergen and Weehawken, New Jersey. He studied at Newark College of Engineering and in June, 1962 was awarded simultaneously a B.S. in chemical engineering and a commission in the United States Air Force. Immediately thereafter he was assigned as an Air Force Institute of Technology student at the Pennsylvania State University where he was awarded a B.S. in meteorology in June, 1963. After spending three years as a Weather Officer at Ft. Leonard Wood in Missouri providing weather support for U.S. Army aviation and ground operations, the author received a second Air Force Institute of Technology assignment at the University of Colorado where he received an M.S. degree in Astro-geophysics in January, 1968. After four and a half years at the Air Force Cambridge Research Laboratories as a Solar Research Physicist, he left the Air Force in August, 1972 to pursue Ph.D. studies in the Department of Meteorology at M. I. T.

Publications:

- 1969: On the role of Joule heating as a source of gravity-wave energy above 100 km. J. Atmos. Sci., 26, 210-217 (with W. Blumen).
- 1972: The results of matched patrol telescope systems (Abstract). Bull. Amer. Astron. Soc., 4, 384 (with F. Ward and R. F. Carnevale).
- 1973: Solar flare observations from a pair of matched instruments. Solar Phys., 31, 131-141 (with F. Ward and R. F. Carnevale).